# Obesogenic and diabetogenic effects of high-calorie nutrition require adipocyte BK channels

Julia Illison[1], Lijun Tian[2], Heather McClafferty[2], Martin Werno[3], Luke H. Chamberlain[3], Veronika Leiss[4], Antonia Sassmann[5], Stefan Offermanns[5], Peter Ruth[1], Michael J. Shipston[2], Robert Lukowski[1, §]

[1]Pharmakologie, Toxikologie und Klinische Pharmazie, Institut für Pharmazie, Tübingen, Germany
[2]Centre for Integrative Physiology, College of Medicine and Veterinary Medicine, University of Edinburgh, Edinburgh, UK
[3]Strathclyde Institute of Pharmacy and Biomedical Sciences, Strathclyde University, Glasgow, UK
[4]Department of Pharmacology and Experimental Therapy, Institute of Experimental and Clinical Pharmacology and Toxicology, University Hospital Tuebingen, Tuebingen, Germany
[5]Department of Pharmacology, Max-Planck-Institute for Heart and Lung Research, Bad Nauheim, Germany

[§]**Corresponding author:** Robert Lukowski, Department of Pharmacology, Toxicology and Clinical Pharmacy, Institute of Pharmacy, University of Tübingen, Tel. +49 7071 29 74550, Fax +49 7071 29 2476, E-mail: robert.lukowski@uni-tuebingen.de

**Running Title:** Adipocyte BK protects from overwhelming BW gain

**Keywords and Abbreviations**: *KCNMA1;* large conductance $Ca^{2+}$- and voltage-activated $K^+$ channel (BK); white adipose tissue (WAT), brown adipose tissue (BAT); epididymal WAT (eWAT); interscapular WAT (intWAT); interscapular BAT (intBAT); mesenteric WAT (mesWAT); subcutaneous inguinal WAT (iWAT); 3T3-L1 cells*;* pre-adipocytes (pre-adipo); hormone-sensitive lipase (HSL); interleukin-6 (IL-6); leptin; adiponectin (ADIPOQ); browning; uncoupling protein 1 (UCP1)

**Number of words:** 4766 (max. 4000) (excluding title page, abstract, research design and methods**,** acknowledgments, references, and table/figure legends)

**Number of words (abstract):** 256 (max. 200)

**Number of references:** 61 (max. 50)

**Page count:** 31

**Abstract**

Elevated adipose tissue expression of the $Ca^{2+}$- and voltage-activated $K^+$ (BK) channel was identified in morbidly obese men carrying a *BK* gene variant supporting the hypothesis that $K^+$ channels affect metabolic responses of fat cells to nutrients. To establish the role of endogenous BKs for fat cell maturation, storage of excess dietary fat and body-weight (BW) gain we studied a gene-targeted mouse model with a global ablation of the *BK* channel ($BK^{L1/L1}$) and adipocyte-specific *BK*-deficient ($adipoqBK^{L1/L2}$) mice. Global *BK* deficiency afforded protection from high-fat-diet (HFD) induced BW gain and excessive fat accumulation. Expansion of white adipose tissue-derived epididymal $BK^{L1/L1}$ pre-adipocytes and their differentiation to lipid-filled mature adipocytes *in vitro*, however, were improved. Moreover, BW gain and total fat masses of usually super-obese *ob/ob* mice were significantly attenuated in the absence of *BK* together supporting a central or peripheral role for BKs in the regulatory system that controls adipose tissue and weight. Accordingly, HFD-fed $adipoqBK^{L1/L2}$ mutants presented with a reduced total BW and overall body fat mass, smaller adipocytes and reduced leptin levels. Protection from pathologic weight gain in the absence of adipocyte BKs was beneficial for glucose handling and related to an increase in body core temperature due to higher levels of uncoupling protein 1 as well as low abundance of the pro-inflammatory interleukin-6 as a common risk factor for diabetes and metabolic abnormalities. This suggests that adipocyte BK activity is at least partially responsible for excessive BW gain under high-caloric conditions suggesting BK channels as promising drug targets for pharmacotherapy of metabolic disorders and obesity.

**Introduction**

Obesity is caused by high calorie intake, typically derived from dietary fats or sugars. Over time, an imbalance between nutrient consumption and burning of calories leads to a massive increase in fat mass, which among other factors is a major cause of insulin resistance and diabetes (1; 2). Additionally, genetic mutations may cause excessive lipid accumulation and thereby a morbid gain in body weight (BW) emphasizing the multifactorial etiology of chronic excessive weight gain (3; 4). It has become increasingly clear that a variety of $K^+$ ion channels *i.e.* $K^+$ channels expressed within the brain and in the periphery, possibly by complex effects on appetite and satiety, energy expenditure, glucose balance and/or fat cell function, are involved in the patho-physiology of obesity and related disorders (5). Accordingly, a genome wide association study recently identified the human *KCNMA1* gene, encoding for the pore forming subunit of the large-conductance $Ca^{2+}$-activated $K^+$ channel (BK), as a novel susceptibility locus for obesity (6). *BK* channel mRNA levels in variant-carriers were significantly increased in white adipose tissue (WAT) and adipose tissue-derived cells, suggesting a pathogenic role for fat cell BK on metabolism. Others reported electrophysiological evidence for BK channels in human pre-adipocytes and BK knock-down, or its pharmacological inhibition, further revealed a possible link between channel activity and proliferative capacity of these cells (7), whereas $Ca^{2+}$-activated $K^+$ channels of the IK type seem to be dominant in the widely-studied murine pre-adipocyte model 3T3-L1 (8). Because both peripheral and central organs, involved in the control of metabolism, express BK it is, however, difficult to estimate the impact of pre-adipocyte BKs on fat cell formation and adiposity *in vivo*. For example, a direct modulation of BK by fatty acids and their metabolites seems to provide a possible link between lipid-mediated effects on the channel and altered vascular functions in hypertriglyceridemia secondary to obesity (9-13). Previous analyses of global *BK* knock-out mice imply that both glucose-induced insulin secretion and endocrine output from the hypothalamic-pituitary-adrenal (HPA) axis, require endogenous BK channels (14; 15). However, it has not been determined whether these dysregulations in β-cell or HPA function caused metabolic abnormalities *in vivo* (16). Moreover, several studies find BK promote inhibitory effects of leptin signaling, *via* PI3-kinase in hippocampal neurons (17) and in mouse chromaffin cells (18), suggesting that neuronal circuits controlling appetite and energy expenditure may also depend on functional BK. A malfunction of neuronal circuits has been widely appreciated as causing excessive fat storage (19) and a number of studies, indeed, found evidence for BK in brainstem, different hypothalamic nuclei, parts of

the cortex and limbic system, hence in brain regions that are implicated in the central control of food intake, appetite and energy expenditure (20; 21).

The recent discovery of functional channels with properties similar to BK in fat cell progenitors (7) together with the link between high fat cell *BK* mRNA expression levels and morbid adiposity (6) suggest that BK activity in the adipose tissue plays, yet to be discovered, physiologically and pathophysiologically important roles for weight control. In order to establish endogenous BK channels as potential modulators of fat deposition and excessive weight gain we herein assessed the susceptibility of global and adipocyte-specific *BK* mouse mutants towards genetic- and dietary-induced causes of adiposity. Our approach to validate BK as a novel player in the response to obesogenic factors *in vivo* should also direct future studies on the pharmacotherapy of adiposity and related disorders.

## Research design and methods

**Animals and diets.** All animal experiments were performed with permission of the local authorities and conducted in accordance with the German legislation on the protection of animals. Animals were housed in cages under controlled environmental conditions with temperatures maintained between 21-24°C, humidity at 45-55% and 12h light-dark-cycle.

Global *BK* channel deficient mice (genotype: $BK^{L1/L1}$), heterozygous (genotype: $BK^{L1/+}$) and wildtype littermates (genotype: $BK^{+/+}$) on a C57BL/6N background were generated and maintained at the Institute of Pharmacy, Department of Pharmacology, Toxicology and Clinical Pharmacy, University of Tübingen as described previously (22). To produce $BK^{L1/L1}$ mice which are also unable to produce functional leptin (genotype: $BK^{L1/L1}$; $B6.V\text{-}Lep^{ob/ob}$ ($BK^{L1/L1}$; *ob/ob*)) $BK^{L1/+}$ animals were crossed to mice carrying a heterozygous mutation of the leptin-gene $B6.V\text{-}Lep^{+/ob}$ *J* (*ob*/+) obtained from Charles River, Germany. Intercrossing of double-heterozygous animals (genotype: $BK^{L1/+}$; $B6.V\text{-}Lep^{ob/+}$ ($BK^{L1/+}$; *ob*/+)) produced homozygous obese $BK^{L1/L1}$; *ob/ob,* obese $BK^{+/+}$ (genotype: $BK^{+/+}$; $B6.V\text{-}Lep^{ob/ob}$ ($BK^{+/+}$; *ob/ob*)), lean $BK^{L1/L1}$ ($BK^{L1/L1}$; $B6.V\text{-}Lep^{+/+}$ ($BK^{L1/L1}$; +/+)) and lean $BK^{+/+}$ ($BK^{+/+}$; $B6.V\text{-}Lep^{+/+}$ ($BK^{+/+}$; +/+)) offspring from the same litters. In order to obtain tissue-specific mutants lacking *BK* in various adipocyte populations heterozygous *BK* mice ($BK^{L1/+}$) on C57BL6 background, carrying a tamoxifen inducible adipose tissue-specific Cre recombinase (genotype: $adiponectin\text{-}CreERT2^{tg/+}$) under control of the adiponectin promoter (23), were first mated to homozygous floxed *BK* animals (genotype: $BK^{L2/L2}$). Adipocyte-specific controls (genotype: $adiponectin\text{-}CreERT2^{tg/+}$; $BK^{+/L2}$ ($adipoqBK^{+/L2}$)) and pre-mutant BK animals (genotype: $adiponectin\text{-}CreERT2^{tg/+}$; $BK^{L1/L2}$ ($adipoqBK^{L1/L2}$)) derived from this breeding were injected with tamoxifen (1 mg/d) for 5 consecutive days to induce Cre-mediated recombination at an age of 8 weeks (Fig. 3 and Fig. 4C-H) or 19 weeks (Fig. 4I).

The specificity and efficiency of the *adiponectin-CreERT2*-derived recombination was supported by studying double fluorescent ROSA26-Tomato reporter mice (genotype: $ROSA26^{mTomato/mEGFP}$ ((*tom*/+)) obtained from Charles River, Germany (24) expressing the adipoqCreERT2 transgene (genotype: $adiponectin\text{-}CreERT2^{tg/+}$; $ROSA26\text{-}Tomato^{tom/+}$; ($adipoq^{tg/+}$; *tom*/+). Double-transgenic animals were either injected with tamoxifen for 5 days as described to induce recombination of the reporter allele *i.e.* a switch from cell membrane-localized red fluorescence to green fluorescence proteins or received solvent. Genotyping was performed using specific primers to identify the Cre transgene (23), the single nucleotide mutation in the leptin gene (according to a protocol for Stock Number: 000632 by The Jackson Laboratory) and the L1, L2 and wild-type alleles of the BK on DNA samples

obtained either from different fat depots, control tissue or tail-tip biopsies from mice that were left untreated or received tamoxifen as described previously (22).

Prior to the different research diets, all experimental mice received tap water and a commercial chow obtained from Altromin, Germany ad libitum. Dietary feeding trials were performed in male mice that were allowed to adapt to a defined control-diet (CD) formulation containing 10% of calories due to fat for two weeks prior the long-term feeding experiments. With 10 weeks of age experimental mice either received a high-fat-diet (HFD) containing 45% or 60% of calories due to fat or were continued to feed the CD for another 18 weeks. Progressive body weight gain in the monogenetic model of obesity was monitored between 4 and 24 weeks of age on normal chow diet.

**Food intake and body core temperature measurements**

The core body temperature and the locomotor activity were measured by using a telemetry setup (ETA-F10 with the two-lead ECG transmitters of the implant removed because they were not required for monitoring the activity and temperature; Data Sciences, Inc.). The surgical procedure was described previously (25). In brief, anesthesia was induced by a 4% isoflurane in oxygen inhalation and was then maintained with 1-2% isoflurane. By aseptic technique the implants were placed in the peritoneal cavity and the skin was closed with a 5/0 surgical silk. During recovery, mice were placed on a warming pad before they were returned to their home cages for at least 3 days before recordings were started. Activity and body core temperature were assessed continuously for 96 hours in experimental mice that had received the HFD diet for 18 weeks.

Food intake was measured using a non-automated and modified metabolic cage setup. To reduce the environmental stress in the feeding chamber of the metabolic cage mice housed individually were placed on paper bedding that was renewed daily. After two days of acclimatization food consumption was assessed for 4 days using an analytic balance. Foot pellets were replaced every 24 hours. The amount of food consumed by each individual mouse was determined by calculating the weight differences between the initial weight of the pellets and the final pellet weights 24 hours later. Food pieces dropped by the animals on the paper bedding were thoroughly collected and included in the final weight determination. Food intake was assessed in a subset of experimental mice prior the dietary feeding at an age of 10 weeks or after the CD or HFD feeding protocols.

**Growth and maturation of pre-adipocytes *in vitro*.** Pre-adipocytes derived from iWAT or eWAT of 10 week old $BK^{+/+}$ and $BK^{L1/L1}$ mice were isolated by an established collagenase liberation protocol (26). Upon 50 min of digestion in Collagenase type I/HEPES buffer at 37°C, $2x10^4$ or $5x10^4$ cells/cm² from iWAT or eWAT were plated in DMEM-Ham's F12 with 5% FCS, respectively. At 90-100% cell confluency maturation was induced by addition of induction medium containing insulin (170 nM), dexamethasone (1 µM), isobutylmethylxanthin (500 µM) and indomethacine (30 µM) to eWAT cultures. Differentiation of iWAT pre-adipocytes was stimulated by adding rosiglitazone (2.5 µM) and triiodothyronine (1 nM) to the eWAT induction medium. After 48h of induction the medium was exchanged by insulin (170 nM) containing medium in DMEM-Ham'sF12 with 10% FCS for another 48h, followed by maintenance medium (DMEM-Ham'sF12 with 10% FCS). Maintenance medium was changed every second day until cells were mature, usually 14 to 16 days after plating. Triglyceride-incorporation was detected by Oil-red-O (ORO) staining. ORO-content was quantified by photometry using the Implen-system at 518 nm. Digital images of the maturation process were acquired using AxioVision software version 4.8 (Carl *Zeiss, Jena, Germany).* Cell-growth and proliferation assays were analyzed in real-time using the xCELLigence impedance setup (OMNI life science, Bremen, Germany) during the first 60 hours upon plating in DMEM-Ham'sF12 with 5% FCS medium. Data was acquired and analyzed using the RTCA software version 1.2.1 (ACEA Biosciencis Inc.).

**Electrophysiological recordings.** The conventional whole-cell mode of patch clamp electrophysiology was used to analyse BK currents in undifferentiated and differentiated 3T3-L1 cells as well as from pre-adipocytes and induced matured adipocytes prepared from primary cultures of mouse eWAT. The pipette solution contained 140 mM KCl, 10 mM HEPES, 30 mM Glucose, 1 mM BAPTA, 2 mM MgCl and free calcium buffered to 0.5µM at pH 7.2. The standard bath (extracellular) solution contained (in mM): 140 mM NaCl 5 mM KCL 10 mM HEPES, 20 mM Glucose, 2 mM MgCl and 1 mM CaCl and pH was adjusted to 7.4. Electrophysiological recordings were performed at room temperature (18-22°C) using pCLAMP 9 (Molecular Devices) with a sampling rate of 10 kHz and filtered at 2 kHz. Patch pipettes were fabricated from borosilicate glass (Garner) with resistances between 2-3 MΩ. Drugs were applied to cells using a gravity perfusion system with a flow rate of 1-2 ml/min to minimise flow-induced artefacts. For analysis of BK currents, the BK channel specific blocker paxilline (1µM) was applied and the paxilline-sensitive outward current analysed at the membrane voltages indicated in the respective figure legends.

**Adipose tissue histology.** For histological examination tissues were fixed in 4% paraformaldehyde for 1.5 hours directly after harvesting and were then embedded in NEG 50™ (Richard-Allan Scientific, Thermo Scientific) for sectioning following sucrose-gradient cryoprotection. Serial 14-µm cryo-sections of different WAT depots were prepared using a HM 560 cryostat (Thermo Scientific, Waltham, USA) and stored at -80°C until further processing. To determine the size of the fat cells prior to and after different diets their perimeter was determined in digital images of the iWAT depot using the AxioVision software package version 4.8 (Carl *Zeiss, Oberkochen, Germany)*. The uncoupling protein 1 (UCP1) expression pattern was compared between iWAT cryo-sections obtained from HFD-fed *adipoqBK*$^{L1/L2}$ and *adipoqBK*$^{+/L2}$ mice using a commercial antibody (Santa Cruz, Dallas, USA) (dilution 1:400). BK immunodetection was performed in iWAT and eWAT sections derived from 10-week old global and adipocyte-specific BK mutants and control litters using a primary antibody, specific for the BK channel alpha subunit (dilution 1:1000) and hormone-sensitive lipase (HSL; dilution 1:400) according to a previously published protocol (27). In brief, antigen-antibody-complexes were detected by a fluorescense-labeled secondary antibody (AlexaFluor®568; anti-rabbit) (dilution 1:500) using the AxioCam MR system (Carl Zeiss, Oberkochen, Germany*)* or by appropriate secondary antibodies conjugated to horseradish peroxidase (dilution 1:500).

**Adipose tissue mass and total body composition.** To determine total fat mass and individual mass of different depots fat pads were dissected unfixed upon dietary-feeding then weighed, immediately immersed in liquid nitrogen and finally stored at -80°C for further analysis. For total body-composition analysis total body weight was determined prior and after drying the corpse for 24 hours at 85°C. Water content was calculated as difference between dry and total weight. Fat-content was determined in dried corpses using the Soxhlet procedure according to a previously published protocol (28).

**Blood parameters and glucose tolerance test.** Blood was collected from mice prior to or after dietary feeding. Leptin, IL-6 and adiponectin levels were measured in serum samples with mouse immunoassay kits (Merck Millipore, Darmstadt, Germany) according to manufacturer's instructions. Blood glucose was determined using the GlucoCheck advance system (TREND Pharma GmbH, Saalfeld/Saale, Germany) immediately before i.p. glucose challenge (2 g/kg of body-weight) as well as 15, 30, 60 and 120 min after the injection in

over-night fasted mice. At each time additional blood (25 µl) was collected via the tail vein for subsequent insulin determination. Plasma-Insulin was measured using the Ultra Sensitive mouse Insulin ELISA (Mercodia, Uppsala Sweden), according to manufacturer's instructions.

**mRNA expression analysis.** Total mRNA was extracted from WAT samples by a guanidineisothiocyanat-phenol-chloroform extraction protocol using PegGold RNA Pure (Peqlab Biotechnologie, Erlangen, Germany) according to the manufacturer's instructions. Following DNase treatment for 30 min to remove traces of genomic DNA, RNA samples were quantified and 0.5 µg RNA were used to generate cDNA using the ISRIPT cDNA synthesis kit (Bio-Rad, Hercules, USA). Quantitative real-time PCR was performed in triplicates using the comparative $2^{-\Delta C(t)}$ method, with C(t) indicating the cycle number at which the signal of the PCR product crosses the threshold, set within the exponential phase of the detected fluorescence signal. BK- and IL-6-levels were normalized to β-actin to determine their relative quantitates. The respective primer sequences designated were: BK forward: 5'-GAC GCC TCT TCA TGG TCT TC -3', BK reverse: 5'-TAG GAG CCC CCG TAT TTC TT-3'; IL-6 forward: 5'- CTT CAA CCA AGA GGT AAA AG -3', IL-6 reverse: 5'-CCA GCT TAT CTG TTA GGA GAG -3'. For extraction of total mRNA from 3T3-L1 cells or pre-adipocytes and differentiated adipocytes in culture the Roche High pure mRNA extraction kit was used according to the manufacturer's instructions following shearing of cells in lysis buffer using a 25G needle. Following DNase treatment as above 0.25 µg RNA were used to generate cDNA using the Roche Transcriptor Hi-Fidelity cDNA synthesis kit with random hexamers and oligo-dT used at a 2:1 ratio. qRT-PCR was performed using the comparative $2^{-\Delta\Delta C(t)}$ method as above with mRNA levels normalized to Ipo8. The respective primers were: BK forward: 5'-GTC TCC AAT GAA ATG TAC ACA GAA TAT C; BK reverse primer: 5'-CTA TCA TCA GGA GCT TAA GCT TCA CA; GLUT4 using the Quantitect Assay (Mm_Slc2a4_2_SG) and Ipo8 using Quantitect assay (Mm_Ipo8_2_SG) from Qiagen.

**3T3-L1 culture and differentiation.** Undifferentiated (UD) 3T3-L1 fibroblasts were maintained in Dulbecco's modified Eagle's Medium (DMEM) containing 10% fetal bovine serum (FBS) and 1% penicillin/streptomycin at 37°C at 10% $CO_2$ and passaged every 4 days after reaching 60-80% confluency. Differentiation was initiated in confluent monolayers in DMEM/FBS containing 1µg/ml insulin, 0.25µM dexamethasone, 1µM troglitazone and 500µM IBMX for 3 days followed DMEM/FBS containing 1µg/ml insulin and 1µM troglitazone. After 3 days cell medium was replaced with DMEM/FBS and medium refreshed

every 3 days until differentiated cells (DF) were analysed (typically 10-14 days after initiation of differentiation).

**Immunoblot analysis of iWAT and 3T3-L1 derived protein lysates.** Inguinal WAT was dissected and processed as described in order to generate total protein lysates for subsequent immunoblot analyses (27). Total protein was obtained from undifferentiated and differentiated 3T3-L1 fibroblasts. Separation of the proteins by molecular weight was done by gel electrophoresis using 12% SDS gels. For immunodetection primary UCP1 (Santa Cruz, Dallas, USA) (dilution 1:1000), Glyceraldehyde-3-phosphate dehydrogenase (GAPDH, dilution 1:1000) (Cell Signaling), glucose transporter type 4 (GLUT4, 1:1000) (generous Gift from Gwyn Gould, Glasgow, UK), BK (1:1000) (NeuroMab, UC Davis, USA) and β-actin (1:500) (Sigma-Aldrich, St. Louis, USA) antibodies were used.

**Statistical analysis.** Statistical analysis was performed on experimental data using a two-tailed student's t-test for paired or unpaired comparison or ANOVA with post-hoc Dunnett's test for multiple comparisons where appropriate. All data are presented as mean ± SEM. For all tests, p-values less than 0.05 were considered as significant: $P<0.05$ (*), $P<0.01$ (**), $P<0.001$ (***).

**Results**

Body weight (BW) gain was investigated in global BK-deficient ($BK^{L1/L1}$) and age- and litter-matched male wild-type mice ($BK^{+/+}$) (Fig. 1A) receiving either a purified low-fat control (CD) or a high-fat diet (HFD). Prior to the different diets we observed a small but highly significant ($P<0.001$) difference in the BWs between the two genotypes as previously reported (29; 30). Starting with 5 weeks of HFD feeding, however, a substantial weight gain in male $BK^{+/+}$ mice became apparent resulting in a total BW gain of 16.44 ± 0.83 g for $BK^{+/+}$ mice at the end of a 18 weeks HFD feeding protocol (Suppl. Fig. 1A), whereas $BK^{L1/L1}$ mutants gained 8.37 ± 0.45 g in the same observation period. Importantly, the differences in BW gain of $BK^{L1/L1}$ mutants were about than 10 % for CD (33.34 ± 2.38%) and HFD (44.26 ± 2.68%) fed groups, whereas the respective difference in the diet induced BW gain for $BK^{+/+}$ mice was 27.76% (Suppl. Fig. 1B). Neither daily food intake of $BK^{+/+}$ and $BK^{L1/L1}$ mice under CD- or HFD-fed conditions (Suppl. Fig. 1C) nor the activity or body-temperature of the animals differed significantly (Suppl. Fig. 1D-E) under HFD suggesting that the lean phenotype of the $BK^{L1/L1}$ mice was, at least not primarily, due to abnormal hyperactivity or dysfunctions in central control of peripheral circuits regulating food intake and reward behaviors. Body-composition revealed that the HFD feeding did not affect wet body mass and carcass dry mass but rather stimulated a substantial increase in the total body fat mass in $BK^{+/+}$ mice, whereas the respective body-composition of CD- and HFD-fed $BK^{L1/L1}$ did not differ (Fig. 1B) supporting the notion that the genotype-specific differences in BW upon CD and HFD feeding (Fig. 1A) are largely due to reduced accumulation of fat in the absence of *BK*. Less total body fat mass of CD- and HFD-fed $BK^{L1/L1}$ mice were accompanied by a small but significant shift to lower dry mass values and reduced tibial length (TL) (Suppl. Fig. 1F) both confirmatory for the lower overall body size in the global absence of BK channels (Fig. 1C). Analyses of fat mass-normalized to TL revealed significant weight differences for various white adipose tissue (WAT) depots as well as the interscapular brown adipose tissue (BAT) indicating that the lean phenotype of the $BK^{L1/L1}$ mice was related to a decrease in multiple adipocyte tissue cell populations (Fig. 1D). So far, the data suggest that high-caloric nutrition-induced BW gain requires functional BK channels. Additionally, the reduced TL, in the global *BK* knock-outs is in accordance with previous reports collectively implying a mild growth defect that may contribute, at least partly, to the differences observed between $BK^{+/+}$ and $BK^{L1/L1}$ BW during dietary feeding (30). We next tested whether BK plays a role for the excessive fat accumulation in the monogenic *ob/ob* model of morbid obesity. BW gain (Suppl. Fig. 2A), body-composition (Suppl. Fig. 2B+C) and individual weights of different fat

depots (Suppl. Fig. 2D) were studied in *BK*-negative *ob/ob* double-mutants and age- and litter-matched *ob/ob* controls. In line with the HFD-fed $BK^{+/+}$ and $BK^{L1/L1}$ mice we find that key parameters of the progressively developing super-obese phenotype, including body weight, body-composition and fat depot masses are attenuated in the absence of BK (Suppl. Fig. 2A-D). In contrast, differences in BW gain between lean control mice in the absence (Δ16.83 ± 0.55 g) and presence (Δ15.73 ± 0.55 g) of BK were not significant (p = 0.17). Protection against overwhelming BW gain in the *BK*-deficient *ob/ob* model was related to a consistent effect on total fat masses and non-fat components of the body (Suppl. Fig. 2B). Indeed, a lower initial as well final BW of BK-negative lean and *ob/ob* double-mutant mice (Suppl. Fig. 2A) as well as differences in the mean TL (Suppl. Fig. 2E) suggest that BK plays a role for normal growth development (Suppl. Fig. 2) and morbid obesity resulting from leptin deficiency.

Based on previous reports on the role of $K^+$-channels in adipocytes (6; 7) and our consistent observation of lower fat masses of multiple fat depots (Fig. 1D and Suppl. Fig. 2D) we considered that the protection from overwhelming weight gain was stemming from the adipocyte itself. To address this possibility, we first assessed the *BK* mRNA and protein expression in inguinal and epididymal white adipose tissue (iWAT and eWAT, respectively). Fat pads were studied using primer pairs allowing for specific detection and quantification of *BK* mRNA (Fig. 1E+F). As compared to the internal reference *BK* levels in $BK^{+/+}$ iWAT and eWAT depots were low but reliable amplification was accomplished in all samples tested. Importantly, signal traces detected in the respective fat depots derived from $BK^{L1/L1}$ mice were well in the range of non-specific PCR product formation in the absence of reverse transcriptase (Suppl. Fig. 3A+B). Because adipose tissue is heterogeneous, composed of fat- and non-fat cells, we next examined the cellular distribution of BK channel protein in frozen adipose tissue sections obtained from 10 week old $BK^{+/+}$ and $BK^{L1/L1}$ mice. These analyses revealed evidence for BK in unilocular $BK^{+/+}$ cells, characteristic of white adipocytes, whereas $BK^{L1/L1}$ iWAT and eWAT remained BK-negative (Fig. 1G+H). Importantly, our specific BK antibodies and an antibody for the white fat cell marker hormone-sensitive lipase (HSL) marked the same cells in $BK^{+/+}$ eWAT (Suppl. Fig. 3C) supporting the notion that mature adipocytes express BK channels.

To explore the functional attributes of endogenous BK channels in adipocytes we adopted a previously established protocol of primary culture and differentiation of murine adipocyte

precursor cells (26). Adipocyte differentiation was induced at 90-100% confluence of $BK^{+/+}$ and $BK^{L1/L1}$ precursor cells derived either from eWAT and iWAT depots. Oil-red-O (ORO) incorporation into lipid droplets revealed strong accumulation of lipid-filled adipocyte-like cells under adipogenic maintenance conditions in cell cultures derived from both *BK*-negative and $BK^{+/+}$ eWAT (Fig. 2A-C) and iWAT (Fig. 2D-F). In iWAT-derived cultures we did not observe differences in the adipogenic differentiation among genotypes (Fig. 2D-F), whereas the amount of ORO incorporation was significantly higher in $BK^{L1/L1}$ than $BK^{+/+}$ cultures established from eWAT (Fig. 2A-C) suggesting a depot-specific role for BK on *in vitro* lipid-storage. Moreover, genetic and pharmacological blockade of BK channels enhanced the growth of eWAT-derived pre-adipocytes (Fig. 2G+H).

To further validate differentiated adipocytes from eWAT express functional BK channels, we assayed BK mRNA, protein and ionic currents in the differentiated cultures. BK channel, as well as GLUT4 transporter, mRNA and protein were strongly upregulated in differentiated cells compared to precursor cells (Fig. 2I+J). Importantly, outward potassium currents, sensitive to the specific BK channel blocker paxilline (1 µM), were significantly upregulated in differentiated adipocytes (Fig. 2K). An increase in BK channel mRNA, protein and currents were also observed in the established 3T3-L1 pre-adipocyte cell model following induction of differentiation (Suppl. Fig. 4A-C). In addition, inhibition of BK channels with paxilline increased the growth of 3T3-L1 pre-adipocytes and the amount of ORO incorporation into lipid droplets (Suppl. Fig. 4D+E). Taken together, these data suggest that fat cell BK channels control pre-adipocyte expansion and adipogenic conversion of pre-adipocytes in an adipocyte depot specific manner.

Because homeostasis of mature adipocyte and adipocyte differentiation *in vivo* are distinct from the above studied *in vitro* models, we next studied the lean phenotype by generating an adipocyte-specific BK knock-out mouse model ($adipoqBK^{L1/L2}$). In a first series of experiments we confirmed the tissue-specific recombination efficacy of the recently established adiponectin promotor-driven tamoxifen-inducible CreERT2 mouse model (23) using a two-color fluorescent Cre reporter system (24). Prior to Cre-mediated excision we observed ubiquitous expression of a cell membrane-targeted red fluorescent Tomato (mT) in eWAT, iWAT and all other tissues studied suggesting that the $ROSA^{mT/mG}$ mouse is indeed a global Cre reporter model (Fig. 3A+B and data not shown). Tamoxifen induced Cre-mediated excision of the floxed *mT* was leading to an almost complete switch to green fluorescent protein (mG) expression in eWAT and iWAT fat cells, whereas changes in mT labelling were not observed in various other organs such as brain, skeletal muscle, and liver (data not

shown). High efficiency and specificity of the adiponectin-CreERT2 approach was further confirmed by a *BK* specific primer set designed to identify the three different *BK* alleles *i.e.* wild-type (+), floxed (L2) and knock-out (L1) within one sample. In line with the Cre-reporter assay (Fig. 3A+B) PCR products indicative of a recombination event were only observed in white and brown adipocyte tissues of adiponectin-CreERT2 transgenic $BK^{+/L2}$ mice ($adipoqBK^{+/L2}$), whereas analysis of multiple other cell types and organ systems did not reveal significant Cre activity regardless of whether tamoxifen was applied or not (Fig. 3C). As compared to $adipoqBK^{+/L2}$ controls, eWAT and iWAT *BK* mRNA expression levels were reduced in tissue-specific $adipoqBK^{L1/L2}$ mutants upon tamoxifen application (Fig. 3D). Accordingly, adiponectin-CreERT2 activation by tamoxifen resulted in a nearly complete ablation of the BK protein in the different WAT tissues (Fig. 3E+F). Hence, the adipocyte-specific knock-out model of *BK* should allow us to test the role of fat cell BK channels for BW gain under CD- and HFD-feeding conditions in the absence of changes in satiety or adiposity signals arising from endocrine or neuronal circuits potentially involving hypothalamic BK channels among others. To induce site-specific recombination of the L2 *BK* gene locus, $adipoqBK^{L1/L2}$ mice as well as $adipoqBK^{+/L2}$ control age- and littermates were subjected to the tamoxifen injection 2 weeks prior to the experimental diets *i.e.* a CD or a HFD with 60% of its calories derived from fat (Fig. 4A+B). Consistent with our previous findings in the global $BK^{L1/L1}$ model (Suppl. Fig. 1C), the tissue-specific ablation of BK did not affect the amount of CD or HFD food consumed by the animals at the start or end of the feeding experiment (Fig.4C+D). Starting BWs and BW gain in the CD group were not different between $adipoqBK^{+/L2}$ and $adipoqBK^{L1/L2}$ mice (Fig. 4E+G), whereas lack of adipocyte BK channels afforded partial protection against HFD-induced gain in BW (Fig. 4F+H), an effect that reached the significance level after 4 weeks of HFD-feeding and was maintained until the mice reached their final BWs (Fig. 4F) indicative for a lower susceptibility of $adipoqBK^{L1/L2}$ mutant mice towards high caloric challenges. We next tested whether excess BW gain is also affected by fat cell BK in mice which have already established significant weight gain. To test this, tamoxifen treatment was commenced at an age of 19 weeks when the $adipoqBK^{+/L2}$ control and $adipoqBK^{L1/L2}$ pre- mutants had reached a BW of 32.35 ± 1.05 g and 31.91 ± 0.89 g, respectively. Total BW gain was not different between age-and litter-matched $adipoqBK^{+/L2}$ and $adipoqBK^{L1/L2}$ mice prior to the tamoxifen treatment ($t_{10\text{-}19}$ 8.18 ± 1.00 g for $adipoqBK^{+/L2}$ and $t_{10\text{-}19}$ 7.71 ± 0.76 g for $adipoqBK^{L1/L2}$ (P = 0.7)), whereas upon five repetitive tamoxifen injections the extent of the weight gain showed

a clear tendency towards lower values in *adipoqBK*$^{L1/L2}$ mice (Fig. 4I) ($t_{20\text{-}30}$ 5.33 ± 0.56 g for *adipoqBK*$^{L1/L2}$ and $t_{20\text{-}30}$ 7.40 ± 1.03 g for *adipoqBK*$^{+/L2}$ (P<0.06))

In depth analyses of the individual fat depots (Fig. 5A+G) and the total fat mass (Fig. 5B) did not reveal statistical weight differences between *adipoqBK*$^{+/L2}$ and *adipoqBK*$^{L1/L2}$ fed a CD diet. HFD feeding, however, confirmed protection from excessive fat storage in *adipoBK*$^{L1/L2}$ mice. Interestingly, lack of adipocyte BK was associated with lower total fat masses and lower masses of various fat depots (Fig. 5C-G). Because fat mass is determined by both adipocyte number and size we next studied fat storage at the cellular level. Inguinal WAT cell size was calculated by assessing the cell perimeters in different cryo-sectional areas obtained from *adipoqBK*$^{+/L2}$ and *adipoqBK*$^{L1/L2}$ mice. Prior to the different diets *i.e.* at an age of 10 weeks genotype-specific differences in fat cell size were not detectable in different areas of the iWAT sections (Fig. 6A+C). As compared to *adipoqBK*$^{+/L2}$ fat cells, *BK*-deficient adipocytes were smaller upon CD and HFD feeding (Fig. 6A+C). Because enlarged, hypertrophic fat cells in the adipose depot relate to obesity, inflammation and insulin resistance we next tested whether the observed changes in adipocyte morphology (Fig. 6A-C) associates with a more proinflammatory state. Indeed, we find reduced IL-6 mRNA expression in iWAT of HFD-fed *adipoqBK*$^{L1/L2}$ mice and tendentially lower serum IL-6 levels (Fig. 6E; p = 0.11). Moreover, HFD-fed *adipoqBK*$^{L1/L2}$ mice exhibited lower serum leptin levels as a marker of body-mass (Fig. 6F), whereas adiponectin concentrations were not different between diets or genotypes (Fig. 6G). In accordance with the markers of inflammation, low adipose tissue mass and fat cell hypertrophy, *adipoqBK*$^{L1/L2}$ mice showed an improved glucose clearance (Fig. 6H) with lower insulin levels (Fig. 6J) upon intra-peritoneal glucose challenge after HFD-feeding, whereas lack of adipocyte BK did not affect glucose handling prior to the feeding protocol (Fig. 6I). Change in cellularity of the iWAT may also be taken as an indicator for accelerated browning to promote energy expenditure which will counter obesity and its metabolic consequences. Lack of fat cell BK resulted in strong induction of the uncoupling protein 1 (UCP1) (Fig. 7A+C) as a hallmark of uncoupled respiration and heat production by brown or brown adipocyte-like fat cells. Higher levels of UCP1 protein under HFD-fed conditions were also reflected by a significant increase in core body temperature during the night (Fig. 7D), whereas during the day, while the mice were sleeping, body temperatures of *adipoqBK*$^{L1/L2}$ and *adipoqBK*$^{+/L2}$ mice were lower suggesting a reduced burning of stored fats with no apparent differences between the two genotypes (Fig. 7D).

In summary, adipocyte BKs promote fat cell size and fat pad mass *in vivo*. Adipocyte tissue growth in the presence of endogenous BK channels was related to a noninfectious activation of adipose tissue inflammation and metabolically unfavourable effects on fat cell functions, which together may result in insulin resistance and amplified HFD-induced adiposity.

**Discussion**

By our combined analysis of different BK channel mutant mouse lines we have uncovered a novel function for adipocyte BKs in fat cell biology and metabolism under different nutritional conditions. We find resistance to HFD-induced BW gain, lower total fat mass and thereby improved glucose handling upon ablation of endogenous BK channels in adipose depots in different parts of the body. These data imply that the development of obesity caused by nutrient excess is promoted by the BK channel (Fig. 4). Accordingly, a previously identified *BK* gene variant was associated with elevated levels of fat cell BK mRNA in morbidly obese human subjects suggesting a causal relationship between the amount of adipocyte BKs and weight gain (6). To the best of our knowledge, BK levels in other organ systems of the affected patients have not been assessed; therefore, it remains unclear if the obesogenic effects attributed to amplified BK expression resulted exclusively from an effect on adipocyte cell function or whether BK channels present in non-adipocyte cells contributed to morbid weight gain. Interestingly, our HFD-fed $BK^{L1/L1}$ mutants did not exhibit any changes in dietary food consumption or body temperature (Suppl. Fig. 1C+D), whereas the respective fat-cell specific mutants exhibited a lean phenotype that was related to an increase in UCP1 levels and energy expenditure (Fig. 7). It therefore seems tempting to speculate that BK channels in the brain or other non-fat cells dot no play a role for the chemical and neural signals regulating calorie intake and/or energy expenditure and thereby body composition. For several reasons, however, we find it is too early to draw such conclusions:

*i.*) Our previous analyses of the global $BK^{L1/L1}$ mouse model revealed multiple defects in various systems of these animals including in β-cells (15), the HPA-axis (14) and cerebellar neurons (29), which separately or together could affect energy balance and BW development. For example, lack of cerebellar BK channels in Purkinje cells, among other deficits, was shown to cause motor learning impairment and signs of ataxia with the latter being related to muscle shivering and trembling (29), a common cause for increased energy expenditure. Irrespective of the dietary fat content we did not observe an increase in the body core temperatures of $BK^{L1/L1}$ mice (Suppl. Fig. 1D) suggesting that their very low body-fat content (Fig. 1) allow them to keep body temperature at physiological levels. Potential changes in body temperature regulation *i.e.* adjustments due to changes in non-/shivering thermogenesis may be superimposed by the loss of heat in $BK^{L1/L1}$ mutants. Yet, $BK^{L1/L1}$ mice present with a lean phenotype with CD and HFD feeding regimes and we observed a lower propensity of the *BK/ob* double mutants to accumulate excessive body weight and fat mass. This suggests that the global lack of BK channels for the entire lifespan prevents the excessive BW gain, an

effect that was more obvious in the presence of genetic or nutritional risk factors for obesity development. In this complex mouse model, a dysregulation of multiple pathways (in fat cells, hypothalamus, liver, sympathetic neurons, β-cells, etc.) involving BK may be related to this phenotype.

*ii.)* The protection in terms of BW gain and fat accumulation was less pronounced in adipocyte specific BK knock-out groups as compared to the $BK^{L1/L1}$ or *BK/ob* double mutant models (compare Fig. 1A, Suppl. Fig. 2A and Fig. 4F) implying non-fat cell BKs are also important for weight control *in vivo.* Indeed, dietary-related changes in energy expenditure involving, for example, hypothalamic control mechanisms may be positively or opposingly regulated by BK channels of neuronal nuclei that respond to satiety or hunger signals. Lack of GIRK4, a G protein-gated inwardly rectifying $K^+$-channel, in mice, for instance, resulted in late onset obesity through hypothalamic mechanisms (31), whereas ATP-sensitive $K^+$ channel ($K_{ATP}$) knock-out mice showed hyperphagia but were resistant to HFD induced BW and visceral fat mass gain (32). Along these lines, $K_{ATP}$ conductance in diet-induced obesity has been reported in pro-opiomelanocortin positive nuclei of the hypothalamus, and neuronal excitability and thereby the release of peptides that control food intake and BW were sensitive to central $K_{ATP}$ inhibition (33). In addition to $K_{ATP,}$ BK channels have been shown to modulate the excitability of hypothalamic neurons in response of insulin and leptin under physiological conditions (34) suggesting they may be involved in central circuits regulating BW *via* energy intake and expenditure. Given the complexity of the different metabolic pathways future studies are needed to clarify the functional roles of hypothalamic and other non-fat cell BK channels in adiposity and thereby the mechanism(s) underlying the lean phenotype of $BK^{L1/L1}$ mice. Resistance to genetic and diet-induced models of obesity *i.e.* hypothalamic-driven obesity has also been reported in mice with a Shaker family voltage-dependent $K^+$ channel gene disruption in *Kv1.3* (35; 36), further highlighting the importance of $K^+$ channels for the hypothalamic-regulation of BW (37). More recently, however, therapeutic benefits on obesity and insulin resistance upon Kv1.3 inhibition by using a blocker which was unable to cross the blood–brain barrier have been attributed to peripheral mechanisms stemming from changes in liver and WAT metabolism and brown adipose tissue (38). Obviously, peripheral and central $K^+$-channels affect the development of adiposity.

Studying adipocyte-specific *BK* knockout mice, we did not find any evidence for tamoxifen-induced recombination in different brain regions including the hypothalamus and other tissues involved in total body metabolism such as muscle or liver (Fig. 3) suggesting that partial protection from diet-induced obesity (Fig. 4F) is resulting from the lack of BK channels in

adipocytes (Fig. 3). Further, we observed amplified BK expression and currents with adipogenic differentiation of both mouse adipocytes from eWAT fat cell precursors as well as in the pre-adipocyte 3T3-L1 cell line (Fig. 2K and Suppl. Fig. 4C). Pharmacological blockade of BK channels stimulated both growth and lipid incorporation supporting a role of BK channels as regulators of cell cycle progression in human pre-adipocytes (7). By assessing BK-deficient eWAT and iWAT derived pre-adipocytes *in vitro*, however, we recognized fat depot specific functions for endogenous BK channels potentially involved in control of cell growth and lipid accumulation (Fig. 2). Because adiposity is usually induced through hypertrophic expansion of existing adipocytes leading to dysfunctional cells, an increase in the number of fat cells *i.e.* hyperplasia is proposed as mechanism that preserves metabolic fitness (39). Accordingly, lower levels of the pro-inflammatory cytokine IL-6 (Fig. 6D+E), significantly lower body weight (Fig. 4F), and smaller iWAT cell size together support the notion that lack of BK leads to the production of more "healthy" adipocytes that may afford protection against excessive BW gain thereby maintaining a regular response to the action of insulin. Reportedly, adipocytes produce and release IL-6 (40). In obesity the fraction of adipose-tissue derived IL-6 may promote a chronic state of low-grade inflammation affecting metabolism and development of insulin resistance (41). In comparison to *adipoqBK*$^{L1/L2}$ mutant mice we find higher IL-6 adipose tissue mRNA ($p < 0.05$) and non-significantly elevated serum levels ($p = 0.11$) in HFD-fed *adipoqBK*$^{+/L2}$ control mice, hence, it appears that fat cell BK channel activity is positively related to the adipose tissue IL-6 pathway providing a link between BK and obesity-related co-morbidities such insulin resistance (Fig. 6D+E and H). Interestingly, high plasma and adipose tissue levels of IL-6 were previously reported for the *ob/ob* mouse model (42), suggesting that BK channels may interfere with both, the genetic- and dietary-induced causes of adiposity by an IL-6-dependent mode of action. Along the same lines, HFD over-nutrition of *adipoqBK*$^{L1/L2}$ mice revealed lower total fat mass and smaller fat cells in iWAT depots. Of note, iWAT cells and depots differed in size and mass only *in vivo* (Fig. 6), whereas in pre-/adipocyte cultures originating from iWAT pads we did not detect differences in terms of various adipogenic parameters (Fig. 2). The reason for this apparent discrepancy is unclear although several mechanisms could be involved. First, *in vivo* the adipocyte-specific lack of BK channels results in a decrease of the iWAT but not eWAT depot fat mass. A "normal" mass of the *adipoqBK*$^{L1/L2}$ eWAT depot *in vivo* (Fig. 5A+C) may result from direct effects of the BK on the lipid storage and cell growth capacities and both parameters were augmented in the respective *BK*$^{L1/L1}$-derived fat cells *in vitro* (Fig. 2A-C and G+H). In contrast, a lower eWAT depot mass in the global BK knockouts (Fig. 1D) may

result from dysregulation of BK-dependent mechanisms in non-adipocytes. Interestingly, our observations in HFD-fed *adipoqBK*$^{L1/L2}$ and *adipoqBK*$^{+/L2}$ mice imply a small but significant increase of approx. 0.3°C in the body's core temperature in the absence of fat cell BKs (Fig. 7D), which indicates that these channels are involved in the thermogenic program of adipose cells. Presence of UCP1 in iWAT is characteristic of a process known as browning where this depot acquires brown adipocyte-like catabolic functions (43), and we find the adipocyte-specific ablation of BK channels to result in elevated mRNA (data not shown) and protein levels of iWAT UCP1 (Fig. 7A-C). Burning of stored fats by expansion or activation of BAT or by browning of WAT may result in a metabolically favorable phenotype (44). Accordingly, we observed a large fraction of smaller fat cells in iWAT, lower iWAT and total fat depot weights as well as an improved glucose homeostasis and insulin sensitivity in HFD-fed *adipoqBK*$^{L1/L2}$ mice (Fig. 7A-C and H-J).

Clearly, the mechanistic details underlying the lean phenotype of HFD-fed *adipoqBK*$^{L1/L2}$ mutants require future investigation. In general, it is widely accepted that BK channels are activated either by a raise in intracellular $Ca^{2+}$ ($[Ca^{2+}]_i$) or by membrane depolarization. $[Ca^{2+}]_i$ dynamics have a multifaceted role for brown adipocyte-like functions and for the formation of mature fat laden adipocytes (45-52), however relatively little is known about $Ca^{2+}$ signaling in white and brown adipocytes despite its suggested importance (53). Yet, efflux of $K^+$ *via* BK in non-excitable cells such as adipocytes may serve as a positive regulator for $Ca^{2+}$-entry as well as a number of $Ca^{2+}$-dependent processes, whereas in excitable cells BK is usually part of a negative feedback loop limiting influx of $Ca^{2+}$ via voltage-dependent $Ca^{2+}$ channels (54). Recently, transient receptor potential vanilloid 4 (TRPV4) channels have been identified as a major feature of the influx of extracellular $Ca^{2+}$ into fat cells (55). TRPV4 appears to negatively regulate the thermogenic and proinflammatory programs in adipocytes and mice with a TRPV4 ablation were protected from diet-induced obesity, hence TRPV4 deficiency results in a phenotype very similar to that caused by adipocyte-specific BK ablation. A functional coupling of BK and TRPV4 was reported in different systems (56; 57). Although this paper did not examine this link, we hypothesize that BK may suppress the acquisition of brown adipocyte-like features in white fat cells by an effect on the $Ca^{2+}$-entry and subsequent signaling pathways involving TRPV4 or other $Ca^{2+}$-permeable members of the large TRP channel protein family (50; 51; 58).

Finally, BK channels are common targets of various intracellular signaling molecules including cyclic guanosine-3′,5′-monophosphate (cGMP) and cyclic adenosine-3′,5′-monophosphate (cAMP) (59; 60). It is well established that both, cAMP and cGMP pathways,

play, among others processes, differential roles in lipolysis, browning of WAT and brown fat cell thermogenesis (44; 61), which should allow for complex adjustments of BK function in the different fat depots *in vivo* under patho-/physiological conditions.

Together, the presented data show that loss of fat cell BK channels supports the browning of fat cells to enhance thermogenesis in response to nutritional excess thereby limiting excessive weight gain. Targeting fat cells with BK channel inhibitors may thus hold potential to reduce pathologic features of excessive weight gain and related disorders.

**Acknowledgments**

The authors thank Clement Kabagema-Bilan, Isolde Breuning, Michael Glaser, and Katrin Junger (all from the Department of Pharmacology, Toxicology and Clinical Pharmacy, Institute of Pharmacy, University of Tuebingen, Tuebingen, Germany) for excellent technical help.

**Funding**

The work was in part funded by: The Deutsche Forschungsgemeinschaft (to RL and PR), the Wellcome Trust (to MJS and PR), and Diabetes UK (to MJS and LHC).

**Duality of interest**

No potential conflicts of interest relevant to this study were reported.

**Author Contributions**

*Research design:* PR, MJS, and RL; *conducted experiments:* JI, LT, HM, MW, and MJS; *contributed new reagents, techniques or analytic tools:* LHC, VL, AS, and SO; *data analysis:* JI, MJS, and RL; *wrote or contributed to the writing of the manuscript:* JI, MJS, and RL; *Contributed to discussions*: PR; *approved the final manuscript: all authors.* RL *and* MJS *are the guarantors of this work and, as such, take responsibility for the integrity of the data and the accuracy of the data analysis.*

**References**

1. Gesta S, Tseng YH, Kahn CR: Developmental origin of fat: tracking obesity to its source. Cell 2007;131:242-256
2. Kahn SE, Hull RL, Utzschneider KM: Mechanisms linking obesity to insulin resistance and type 2 diabetes. Nature 2006;444:840-846
3. Choquet H, Meyre D: Genetics of Obesity: What have we Learned? Current genomics 2011;12:169-179
4. Ramachandrappa S, Farooqi IS: Genetic approaches to understanding human obesity. The Journal of clinical investigation 2011;121:2080-2086
5. Sohn JW: Ion channels in the central regulation of energy and glucose homeostasis. Frontiers in neuroscience 2013;7:85
6. Jiao H, Arner P, Hoffstedt J, Brodin D, Dubern B, Czernichow S, van't Hooft F, Axelsson T, Pedersen O, Hansen T, Sorensen TI, Hebebrand J, Kere J, Dahlman-Wright K, Hamsten A, Clement K, Dahlman I: Genome wide association study identifies KCNMA1 contributing to human obesity. BMC medical genomics 2011;4:51
7. Hu H, He ML, Tao R, Sun HY, Hu R, Zang WJ, Yuan BX, Lau CP, Tse HF, Li GR: Characterization of ion channels in human preadipocytes. Journal of cellular physiology 2009;218:427-435
8. Zhang XH, Zhang YY, Sun HY, Jin MW, Li GR: Functional ion channels and cell proliferation in 3T3-L1 preadipocytes. Journal of cellular physiology 2012;227:1972-1979
9. Dopico AM, Bukiya AN: Lipid regulation of BK channel function. Frontiers in physiology 2014;5:312
10. Martin P, Moncada M, Enrique N, Asuaje A, Valdez Capuccino JM, Gonzalez C, Milesi V: Arachidonic acid activation of BKCa (Slo1) channels associated to the beta1-subunit in human vascular smooth muscle cells. Pflugers Archiv : European journal of physiology 2014;466:1779-1792
11. Hoshi T, Tian Y, Xu R, Heinemann SH, Hou S: Mechanism of the modulation of BK potassium channel complexes with different auxiliary subunit compositions by the omega-3 fatty acid DHA. Proceedings of the National Academy of Sciences of the United States of America 2013;110:4822-4827
12. Lynch FM, Withers SB, Yao Z, Werner ME, Edwards G, Weston AH, Heagerty AM: Perivascular adipose tissue-derived adiponectin activates BK(Ca) channels to induce anticontractile responses. American journal of physiology Heart and circulatory physiology 2013;304:H786-795
13. Climent B, Simonsen U, Rivera L: Effects of obesity on vascular potassium channels. Current vascular pharmacology 2014;12:438-452
14. Brunton PJ, Sausbier M, Wietzorrek G, Sausbier U, Knaus HG, Russell JA, Ruth P, Shipston MJ: Hypothalamic-pituitary-adrenal axis hyporesponsiveness to restraint stress in mice deficient for large-conductance calcium- and voltage-activated potassium (BK) channels. Endocrinology 2007;148:5496-5506
15. Dufer M, Neye Y, Horth K, Krippeit-Drews P, Hennige A, Widmer H, McClafferty H, Shipston MJ, Haring HU, Ruth P, Drews G: BK channels affect glucose homeostasis and cell viability of murine pancreatic beta cells. Diabetologia 2011;54:423-432
16. Peters A, Schweiger U, Fruhwald-Schultes B, Born J, Fehm HL: The neuroendocrine control of glucose allocation. Experimental and clinical endocrinology & diabetes : official journal, German Society of Endocrinology [and] German Diabetes Association 2002;110:199-211
17. Shanley LJ, O'Malley D, Irving AJ, Ashford ML, Harvey J: Leptin inhibits epileptiform-like activity in rat hippocampal neurones via PI 3-kinase-driven activation of BK channels. The Journal of physiology 2002;545:933-944

18. Gavello D, Vandael D, Gosso S, Carbone E, Carabelli V: Dual action of leptin on rest-firing and stimulated catecholamine release via phosphoinositide 3-kinase-driven BK channel up-regulation in mouse chromaffin cells. The Journal of physiology 2015;593:4835-4853
19. Schneeberger M, Gomis R, Claret M: Hypothalamic and brainstem neuronal circuits controlling homeostatic energy balance. The Journal of endocrinology 2014;220:T25-46
20. Sausbier U, Sausbier M, Sailer CA, Arntz C, Knaus HG, Neuhuber W, Ruth P: Ca2+ -activated K+ channels of the BK-type in the mouse brain. Histochemistry and cell biology 2006;125:725-741
21. Chang CP, Dworetzky SI, Wang J, Goldstein ME: Differential expression of the alpha and beta subunits of the large-conductance calcium-activated potassium channel: implication for channel diversity. Brain research Molecular brain research 1997;45:33-40
22. Sausbier M, Arntz C, Bucurenciu I, Zhao H, Zhou XB, Sausbier U, Feil S, Kamm S, Essin K, Sailer CA, Abdullah U, Krippeit-Drews P, Feil R, Hofmann F, Knaus HG, Kenyon C, Shipston MJ, Storm JF, Neuhuber W, Korth M, Schubert R, Gollasch M, Ruth P: Elevated blood pressure linked to primary hyperaldosteronism and impaired vasodilation in BK channel-deficient mice. Circulation 2005;112:60-68
23. Sassmann A, Offermanns S, Wettschureck N: Tamoxifen-inducible Cre-mediated recombination in adipocytes. Genesis 2010;48:618-625
24. Muzumdar MD, Tasic B, Miyamichi K, Li L, Luo L: A global double-fluorescent Cre reporter mouse. Genesis 2007;45:593-605
25. Lukowski R, Rybalkin SD, Loga F, Leiss V, Beavo JA, Hofmann F: Cardiac hypertrophy is not amplified by deletion of cGMP-dependent protein kinase I in cardiomyocytes. Proceedings of the National Academy of Sciences of the United States of America 2010;107:5646-5651
26. Jennissen K, Haas B, Mitschke MM, Siegel F, Pfeifer A: Analysis of cGMP signaling in adipocytes. Methods Mol Biol 2013;1020:175-192
27. Leiss V, Illison J, Domes K, Hofmann F, Lukowski R: Expression of cGMP-dependent protein kinase type I in mature white adipocytes. Biochemical and biophysical research communications 2014;452:151-156
28. Leiss V, Friebe A, Welling A, Hofmann F, Lukowski R: Cyclic GMP kinase I modulates glucagon release from pancreatic alpha-cells. Diabetes 2011;60:148-156
29. Sausbier M, Hu H, Arntz C, Feil S, Kamm S, Adelsberger H, Sausbier U, Sailer CA, Feil R, Hofmann F, Korth M, Shipston MJ, Knaus HG, Wolfer DP, Pedroarena CM, Storm JF, Ruth P: Cerebellar ataxia and Purkinje cell dysfunction caused by Ca2+-activated K+ channel deficiency. Proceedings of the National Academy of Sciences of the United States of America 2004;101:9474-9478
30. Soltysinska E, Bentzen BH, Barthmes M, Hattel H, Thrush AB, Harper ME, Qvortrup K, Larsen FJ, Schiffer TA, Losa-Reyna J, Straubinger J, Kniess A, Thomsen MB, Bruggemann A, Fenske S, Biel M, Ruth P, Wahl-Schott C, Boushel RC, Olesen SP, Lukowski R: KCNMA1 encoded cardiac BK channels afford protection against ischemia-reperfusion injury. PloS one 2014;9:e103402
31. Perry CA, Pravetoni M, Teske JA, Aguado C, Erickson DJ, Medrano JF, Lujan R, Kotz CM, Wickman K: Predisposition to late-onset obesity in GIRK4 knockout mice. Proceedings of the National Academy of Sciences of the United States of America 2008;105:8148-8153
32. Park YB, Choi YJ, Park SY, Kim JY, Kim SH, Song DK, Won KC, Kim YW: ATP-Sensitive Potassium Channel-Deficient Mice Show Hyperphagia but Are Resistant to Obesity. Diabetes & metabolism journal 2011;35:219-225
33. Plum L, Ma X, Hampel B, Balthasar N, Coppari R, Munzberg H, Shanabrough M, Burdakov D, Rother E, Janoschek R, Alber J, Belgardt BF, Koch L, Seibler J, Schwenk F, Fekete C, Suzuki A, Mak TW, Krone W, Horvath TL, Ashcroft FM, Bruning JC: Enhanced

PIP3 signaling in POMC neurons causes KATP channel activation and leads to diet-sensitive obesity. The Journal of clinical investigation 2006;116:1886-1901
34. Yang MJ, Wang F, Wang JH, Wu WN, Hu ZL, Cheng J, Yu DF, Long LH, Fu H, Xie N, Chen JG: PI3K integrates the effects of insulin and leptin on large-conductance Ca2+-activated K+ channels in neuropeptide Y neurons of the hypothalamic arcuate nucleus. American journal of physiology Endocrinology and metabolism 2010;298:E193-201
35. Tucker K, Overton JM, Fadool DA: Kv1.3 gene-targeted deletion alters longevity and reduces adiposity by increasing locomotion and metabolism in melanocortin-4 receptor-null mice. Int J Obes (Lond) 2008;32:1222-1232
36. Xu J, Koni PA, Wang P, Li G, Kaczmarek L, Wu Y, Li Y, Flavell RA, Desir GV: The voltage-gated potassium channel Kv1.3 regulates energy homeostasis and body weight. Human molecular genetics 2003;12:551-559
37. Kalra SP, Dube MG, Pu S, Xu B, Horvath TL, Kalra PS: Interacting appetite-regulating pathways in the hypothalamic regulation of body weight. Endocrine reviews 1999;20:68-100
38. Upadhyay SK, Eckel-Mahan KL, Mirbolooki MR, Tjong I, Griffey SM, Schmunk G, Koehne A, Halbout B, Iadonato S, Pedersen B, Borrelli E, Wang PH, Mukherjee J, Sassone-Corsi P, Chandy KG: Selective Kv1.3 channel blocker as therapeutic for obesity and insulin resistance. Proceedings of the National Academy of Sciences of the United States of America 2013;110:E2239-2248
39. Rutkowski JM, Stern JH, Scherer PE: The cell biology of fat expansion. The Journal of cell biology 2015;208:501-512
40. Sopasakis VR, Sandqvist M, Gustafson B, Hammarstedt A, Schmelz M, Yang X, Jansson PA, Smith U: High local concentrations and effects on differentiation implicate interleukin-6 as a paracrine regulator. Obesity research 2004;12:454-460
41. Eder K, Baffy N, Falus A, Fulop AK: The major inflammatory mediator interleukin-6 and obesity. Inflammation research : official journal of the European Histamine Research Society [et al] 2009;58:727-736
42. Harkins JM, Moustaid-Moussa N, Chung YJ, Penner KM, Pestka JJ, North CM, Claycombe KJ: Expression of interleukin-6 is greater in preadipocytes than in adipocytes of 3T3-L1 cells and C57BL/6J and ob/ob mice. The Journal of nutrition 2004;134:2673-2677
43. Bartelt A, Heeren J: Adipose tissue browning and metabolic health. Nature reviews Endocrinology 2014;10:24-36
44. Pfeifer A, Hoffmann LS: Brown, beige, and white: the new color code of fat and its pharmacological implications. Annual review of pharmacology and toxicology 2015;55:207-227
45. Neal JW, Clipstone NA: Calcineurin mediates the calcium-dependent inhibition of adipocyte differentiation in 3T3-L1 cells. The Journal of biological chemistry 2002;277:49776-49781
46. Hu R, He ML, Hu H, Yuan BX, Zang WJ, Lau CP, Tse HF, Li GR: Characterization of calcium signaling pathways in human preadipocytes. Journal of cellular physiology 2009;220:765-770
47. Shi H, Halvorsen YD, Ellis PN, Wilkison WO, Zemel MB: Role of intracellular calcium in human adipocyte differentiation. Physiological genomics 2000;3:75-82
48. Oguri A, Tanaka T, Iida H, Meguro K, Takano H, Oonuma H, Nishimura S, Morita T, Yamasoba T, Nagai R, Nakajima T: Involvement of CaV3.1 T-type calcium channels in cell proliferation in mouse preadipocytes. American journal of physiology Cell physiology 2010;298:C1414-1423
49. Jensen B, Farach-Carson MC, Kenaley E, Akanbi KA: High extracellular calcium attenuates adipogenesis in 3T3-L1 preadipocytes. Experimental cell research 2004;301:280-292

50. Sun W, Uchida K, Suzuki Y, Zhou Y, Kim M, Takayama Y, Takahashi N, Goto T, Wakabayashi S, Kawada T, Iwata Y, Tominaga M: Lack of TRPV2 impairs thermogenesis in mouse brown adipose tissue. EMBO reports 2016;17:383-399
51. Ma S, Yu H, Zhao Z, Luo Z, Chen J, Ni Y, Jin R, Ma L, Wang P, Zhu Z, Li L, Zhong J, Liu D, Nilius B: Activation of the cold-sensing TRPM8 channel triggers UCP1-dependent thermogenesis and prevents obesity. Journal of molecular cell biology 2012;4:88-96
52. Zhang LL, Yan Liu D, Ma LQ, Luo ZD, Cao TB, Zhong J, Yan ZC, Wang LJ, Zhao ZG, Zhu SJ, Schrader M, Thilo F, Zhu ZM, Tepel M: Activation of transient receptor potential vanilloid type-1 channel prevents adipogenesis and obesity. Circulation research 2007;100:1063-1070
53. Worrall DS, Olefsky JM: The effects of intracellular calcium depletion on insulin signaling in 3T3-L1 adipocytes. Mol Endocrinol 2002;16:378-389
54. Yang H, Cui J: BK Channels. In *Handbook of Ion Channels* Zheng J, Trudeau MC, Eds., CRC Press, 2015, p. 227-240
55. Ye L, Kleiner S, Wu J, Sah R, Gupta RK, Banks AS, Cohen P, Khandekar MJ, Bostrom P, Mepani RJ, Laznik D, Kamenecka TM, Song X, Liedtke W, Mootha VK, Puigserver P, Griffin PR, Clapham DE, Spiegelman BM: TRPV4 is a regulator of adipose oxidative metabolism, inflammation, and energy homeostasis. Cell 2012;151:96-110
56. Earley S, Heppner TJ, Nelson MT, Brayden JE: TRPV4 forms a novel Ca2+ signaling complex with ryanodine receptors and BKCa channels. Circulation research 2005;97:1270-1279
57. Fernandez-Fernandez JM, Andrade YN, Arniges M, Fernandes J, Plata C, Rubio-Moscardo F, Vazquez E, Valverde MA: Functional coupling of TRPV4 cationic channel and large conductance, calcium-dependent potassium channel in human bronchial epithelial cell lines. Pflugers Archiv : European journal of physiology 2008;457:149-159
58. Che H, Yue J, Tse HF, Li GR: Functional TRPV and TRPM channels in human preadipocytes. Pflugers Archiv : European journal of physiology 2014;466:947-959
59. Zhou XB, Arntz C, Kamm S, Motejlek K, Sausbier U, Wang GX, Ruth P, Korth M: A molecular switch for specific stimulation of the BKCa channel by cGMP and cAMP kinase. The Journal of biological chemistry 2001;276:43239-43245
60. Zhou XB, Wulfsen I, Utku E, Sausbier U, Sausbier M, Wieland T, Ruth P, Korth M: Dual role of protein kinase C on BK channel regulation. Proceedings of the National Academy of Sciences of the United States of America 2010;107:8005-8010
61. Carmen GY, Victor SM: Signalling mechanisms regulating lipolysis. Cellular signalling 2006;18:401-408

**Figure Legends**

***Figure 1:*** **Global lack of BK channels protects from overwhelming body weight (BW) gain and excessive fat accumulation.**

**(A)** Body weight (BW) increase of $BK^{+/+}$ (blue) and $BK^{L1/L1}$ (red) mice that received a control diet (CD) (n=12-14 mice per time-point; open data points) or 45% high-fat diet (HFD) (n=23-25 mice per time-point, filled data points) for 18 weeks. **(B)** Body-composition of $BK^{+/+}$ and $BK^{L1/L1}$ mice after 18 weeks of dietary feeding was analyzed using the Soxhlet extraction method (n=4-7 mice per genotype). Representative images of **(C)** $BK^{+/+}$ and $BK^{L1/L1}$ mice after 18 weeks of CD- or HFD dietary feeding. **(D)** Fat mass of different white (WAT) and brown (BAT) adipose tissue depots of $BK^{+/+}$ and $BK^{L1/L1}$ mice fed either a CD (n=6-9 mice per fat depot) or HFD (n=9-16 mice per fat depot). Fat masses were normalized to tibia length (Suppl. Fig. 1F) to overcome growth differences between $BK^{+/+}$ and $BK^{L1/L1}$ mice that are not related to gain of body adiposity. Relative mRNA-expression of the BK-channel alpha subunit in **(E)** epididymal WAT (eWAT) and **(F)** subcutaneous inguinal WAT (iWAT) of 10 week old $BK^{+/+}$ and $BK^{L1/L1}$ mice. Glyceraldehyde-3-phosphate dehydrogenase mRNA levels were used as a reference to normalize the data, which are presented as means ± SEM. Statistical difference between the two genotypes is indicated by * P<0.05, ** P<0.01. Representative cryo-sections of **(G)** eWAT and **(H)** iWAT stained for the BK alpha-subunit (upper panels) using a specific BK channel antibody. As negative control frozen tissue sections without the primary BK antibody were processed (lower panels). (G, H) Scale bars represent 200 µm.

Data were analyzed using the 2-way ANOVA test (A) or Student‘s t-test (B, D-F) and are presented as means ± SEM. Statistical difference between the two genotypes is indicated by * P<0.05, ** P<0.01, *** P<0.001. *Abbreviations used:* Epididymal WAT (eWAT); interscapular WAT (intWAT); interscapular BAT (intBAT); mesenteric WAT (mesWAT); subcutaneous inguinal WAT (iWAT).

***Figure 2:*** **Accelerated growth of BK-negative epididymal WAT (eWAT)-derived pre-adipocytes.**

Representative Oil-red-O (ORO) staining of eWAT-derived pre-adipocytes in **(A)** high magnification and **(B)** as overviews screen after 14 days of adipogenic differentiation revealing higher numbers of mature adipocytes in $BK^{L1/L1}$ in comparison to $BK^{+/+}$ cells. **(C)** The increased adipogenic potential in $BK^{L1/L1}$ (red) was confirmed by analyzing ORO-incorporation quantitatively at 518 nm (n=3 independent *in vitro* assays per genotype). **(D, E)**

Representative ORO staining of inguinal WAT (iWAT)-derived pre-adipocytes after 14 days of adipogenic differentiation. Scale bars (A, D) represent 100 µm. **(E, F)** Based on the ORO-incorporation assay maturation of iWAT-derived $BK^{+/+}$ and $BK^{L1/L1}$ pre-adipocytes was not different between the genotypes (n=7-8 independent *in vitro* assays per genotype). **(G)** Representative growth of eWAT-derived pre-adipocytes examined in real-time using an impedance-based setup. Lack of BK channels (red) in eWAT-derived pre-adipocytes resulted in accelerated growth properties at different cell concentrations tested as compared to wild-type cells (blue). **(H)** A pharmacological approach to block the BK channel using 1 µM paxilline confirmed the BK-dependent growth capacity of eWAT-derived pre-adipocytes. **(I)** Up-regulation of GLUT4 and BK channel mRNA and **(J)** protein levels following differentiation of eWAT murine pre-adipocytes (pre-adipo) to adipocytes (adipo) (n=3 independent experiments per group). **(K)** Pre-adipocyte cells display a small paxilline-sensitive (1 µM) outward whole-cell BK potassium current determined under physiological potassium gradients (n=8 cells) that was significantly increased upon adipogenic differentiation for 14 days (n=12 cells).

***Figure 3*: Spatiotemporal ablation of fat cell BK channels using the *adipoqCreERT2*$^{tg/+}$ recombination system.**

Recombination efficiency was determined by a change from red (Cy3-channel) to green (FITC-channel) fluorescence using the *ROSA26-Tomato*$^{tom/+}$ (tom/+) Cre-reporter mouse line. **(A)** Analysis of eWAT and **(B)** subcutaneous iWAT derived from double-transgenic *adipoqCreER*$^{tg/+}$*; ROSA26-Tomato*$^{tom/+}$ (tg/+; tom/+) mice with or without tamoxifen (TAM) injections in comparison to wildtype age-matched littermate male control mice (+/+; +/+). **(C)** Genomic PCR-analysis of the *adipoqCreERT2*$^{tg/+}$-mediated recombination of the pre-mutant BK gene locus in different tissues. PCR products amplified from the loxP-flanked (L2 allele with two loxP sites; two black triangles flanking a closed box), wild type (+ allele; closed black box), and knock-out (L1 allele with one loxP site; one black triangle) alleles of representative *adipoqCreERT2*$^{tg/+}$; $BK^{+/L2}$ (*adipoqBK*$^{+/L2}$) animals. Conversion of the loxP-flanked L2 allele to the L1 allele was only observed in fat cell depots after injecting tamoxifen (+), whereas with saline (-) treatment we did not find evidence for unspecific Cre activity. Recombination was analyzed 14 days after the beginning of tamoxifen or saline injections in 10 weeks old mice. The size of the PCR amplicons were 577 bp, 466 bp and 132 bp for the floxed, WT and knockout allele, respectively. *Abbreviations used:* Pancreas (P); liver (L); hypothalamus (H); bulb (B); cerebellum (C); rest of brain (Br); heart (He); skeletal muscle

(S); duodenum (D); epididymal white adipose tissue (eWAT); subcutaneous inguinal white adipose tissue (iWAT) and brown adipose tissue (BAT); marker (M). **(D)** Quantitative mRNA analysis of the BK mRNA in eWAT and iWAT of TAM-injected *adipoqCreER*$^{tg/+}$; *BK*$^{+/L2}$ control mice (n= 5 for eWAT and iWAT) and age and littermatched *adipoqCreER*$^{tg/+}$; *BK*$^{L1/L2}$ tissue-specific mutants n= 7 for eWAT and n=4 iWAT). Analysis of the frequency and distribution of the adiponectin-CreERT2-mediated recombination after TAM injections in **(E)** eWAT and **(F)** iWAT of *adipoqCreER*$^{tg/+}$; *BK*$^{+/L2}$ (*adipoqBK*$^{+/L2}$) and *adipoqCreER*$^{tg/+}$; *BK*$^{L1/L2}$ (*adipoqBK*$^{L1/L2}$) mice using a specific BK channel antibody (+anti-BK; upper panels). A parallel analysis of serial eWAT and iWAT sections from both genotypes was performed to establish the background fluorescence in the absence of BK-specific antibodies (-anti-BK; lower panels). Scale bars represent 50 µm.

***Figure 4*: Reduced BW gain in *adipoqBK*$^{L1/L2}$ mice receiving a 60% HFD feeding.**

**(A)** Control diet (CD) feeding protocol. Male *adipoqCreER*$^{tg/+}$; *BK*$^{L1/L2}$ (*adipoqBK*$^{L1/L2}$) and *adipoqCreER*$^{tg/+}$; *BK*$^{+/L2}$ (*adipoqBK*$^{+/L2}$) were injected prior to the dietary feeding with tamoxifen (TAM) for 5 consecutive days at an age of 8 weeks, which induced a specific and efficient ablation of the BK channel in various adipose tissues (see also Fig. 3). Upon 2 weeks of adaption to the CD, CD diet feeding was continued or **(B)** mice revived a HFD for 18 weeks (prevention study). In an alternative approach additional groups of *adipoqBK*$^{L1/L2}$ and *adipoqBK*$^{+/L2}$ mice were subjected to the same feeding protocol, but tamoxifen was injected at an age of 19 weeks ($TAM_{19}$) when over-weight has already been established. Food intake of *adipoqBK*$^{L1/L2}$ (red) and *adipoqBK*$^{+/L2}$ (blue) mice were analyzed, using modified metabolic cages as described in the methods section either **(C)** at the beginning (n=4-6 mice per genotype) or **(D)** at the end of the respective dietary feeding (n=3-5 mice per genotype). BW development under **(E)** CD feeding (n=12-20 per genotype/time-point) and **(F)** HFD feeding (n=24-29 mice per genotype/time-point). Difference (ΔBW) between the initial BW (at week 10) and the BW at week 30 in *adipoqBK*$^{L1/L2}$ (red) and *adipoqBK*$^{+/L2}$ (blue) mice under **(G)** CD and **(H)** HFD feeding conditions (n=12-15 per genotype for CD, n=24-26 per genotype for HFD). **(I)** Tamoxifen was injected for 5 consecutive days at an age of 19 week when a HFD-induced BW gain in *adipoqBK*$^{L1/L2}$ (red) and *adipoqBK*$^{+/L2}$ (blue) mice was already established to test the therapeutic potential of WAT BK inactivation (n=17-22 mice per genotype/time-point). The final BW between the two genotypes was significantly different (* $P<0.05$).

***Figure 5:*** **Reduced fat accumulation and smaller fat depots in *adipoqBK$^{L1/L2}$* mice fed a 60% high-fat diet (HFD).**

Mass of different white (WAT) and brown (BAT) adipose tissue depots of male *adipoqBK$^{L1/L2}$* (red) and *adipoqBK$^{+/L2}$* (blue) mice examined after 18 weeks of **(A)** control diet (CD) or **(B)** HFD feeding (n=12-15 per genotype for CD, n=24-26 per genotype for HFD). Body-composition of *adipoqBK$^{+/L2}$* and *adipoqBK$^{L1/L2}$* at an age of 30 weeks **(C)** after CD and **(D)** after HFD feeding. Total body fat was extracted using the soxhlet extraction method (n=3 per genotype for CD, n=4-7 per genotype for HFD). **(E-G)** Representative pictures of *adipoqBK$^{+/L2}$* and *adipoqBK$^{L1/L2}$* mice and selected fat depots after 18 weeks on CD. **(E)** View from back, **(F)** front view with opened abdominal cavity and **(G)** magnification of BAT, eWAT and iWAT. All data were analyzed using the Student‘s t-test and are presented as means ± SEM (* P<0.05). **(E-G)** Scale bars represent 2 cm. *Abbreviations used:* Epididymal WAT (eWAT), interscapular WAT (intWAT), interscapular BAT (intBAT), total interscapular adipose tissue (intAT), mesenteric WAT (mesWAT), subcutaneous inguinal WAT (iWAT) and total investigated adipose depots (total).

***Figure 6:*** **Fat cell hyperplasia and improved glucose handling in *adipoqBK$^{L1/L2}$* mice.**

**(A)** Average cell size of inguinal WAT (iWAT) of male *adipoqBK$^{+/L2}$* and *adipoqBK$^{L1/L2}$* mice after 18 weeks of HFD was examined in serial cryo-sections by measuring the circumference of cells in central and peripheral regions of the respective depots. **(B)** Classification of average cell sizes (as an indicator of adipose cell number) in *adipoqBK$^{+/L2}$* and *adipoqBK$^{L1/L2}$* iWAT, prior diet (PD) and after 18 weeks of control diet (CD) or 60% high-fat diet (HFD) feeding. **(C)** Representative cryo-sections of iWAT derived from *adipoqBK$^{+/L2}$* (blue) and *adipoqBK$^{L1/L2}$* (red) PD or after either 18 weeks of CD or HFD. Scale bars represent 100 µm**.** Relative **(D)** mRNA-expression and **(E)** serum levels of interleukin-6 (IL-6) a marker for adipose tissue inflammation and serum levels of **(F)** adiponectin and **(G)** leptin determined after 18 weeks of CD (open bars) and/or HFD (closed bars) feeding in *adipoqBK$^{+/L2}$* (blue) and *adipoqBK$^{L1/L2}$* (red) mice. Blood-glucose (BG) levels were monitored before as well as 15, 30, 60 and 120 minutes after i.p. injection of 2 g/kg glucose **(H)** after 18 weeks of HFD-feeding and **(I)** prior the respective diet. **(J)** Plasma insulin levels at baseline (0 min) and during the intraperitoneal glucose-tolerance-test (15 to 120 min post injection) in *adipoqBK$^{L2/+}$* (blue, n=6) and *adipoqBK$^{L1/L2}$* (red, n=8) mice after 18 weeks of HFD-feeding. All data (A, D-J) were examined using the Student‘s t-test and are presented as means ± SEM (* P<0.05, ** P<0.01).

***Figure 7:*** **Increased UCP1 levels and body temperature in HFD-fed *adipoqBK$^{L1/L2}$* mice**

(**A**) UCP1 expression analysis (brown staining in left panels) in frozen tissue sections derived from HFD-fed *adipoqBK$^{+/L2}$* and *adipoqBK$^{L1/L2}$* iWAT. As negative control sections derived from the same fat pads were processed in the absence of the primary UCP1 antibody (right panels). (**B**) Representative UCP1immunoblot of iWAT protein lysates derived from HFD-fed *adipoqBK$^{+/L2}$* and *adipoqBK$^{L1/L2}$* mice. Equal loading of the gel was verified by co-detection of glyceraldehyde-3-phosphate dehydrogenase (GAPDH). (**C**) Quantification of the immunoblot data shown in (B). UCP1 protein levels were normalized to the expression of GAPDH in *adipoqBK$^{+/L2}$* (closed blue bars; n=3) and *adipoqBK$^{L1/L2}$* (closed red bars; n=4) iWAT samples. (**D**) Telemetric sensors were used to measure the body core temperature of a subset of *adipoqBK$^{+/L2}$* and *adipoqBK$^{L1/L2}$* mice that received the HFD-feeding. All data (C, D) were assessed using the Student‘s *t*-test and are presented as means ± SEM. * $P<0.05$, ** $P<0.01$.

# Obesogenic and diabetogenic effects of high-calorie nutrition require adipocyte BK channels

Julia Illison[1], Lijun Tian[2], Heather McClafferty[2], Martin Werno[3], Luke H. Chamberlain[3], Veronika Leiss[4], Antonia Sassmann[5], Stefan Offermanns[5], Peter Ruth[1], Michael J. Shipston[2], Robert Lukowski[1, §]

[1]Pharmakologie, Toxikologie und Klinische Pharmazie, Institut für Pharmazie, Tübingen, Germany
[2]Centre for Integrative Physiology, College of Medicine and Veterinary Medicine, University of Edinburgh, Edinburgh, UK
[3]Strathclyde Institute of Pharmacy and Biomedical Sciences, Strathclyde University, Glasgow, UK
[4]Department of Pharmacology and Experimental Therapy, Institute of Experimental and Clinical Pharmacology and Toxicology, University Hospital Tuebingen, Tuebingen, Germany
[5]Department of Pharmacology, Max-Planck-Institute for Heart and Lung Research, Bad Nauheim, Germany

[§]**Corresponding author:** Robert Lukowski, Department of Pharmacology, Toxicology and Clinical Pharmacy, Institute of Pharmacy, University of Tübingen, Tel. +49 7071 29 74550, Fax +49 7071 29 2476, E-mail: robert.lukowski@uni-tuebingen.de

**Running Title:** Adipocyte BK protects from overwhelming BW gain

**Keywords and Abbreviations**: *KCNMA1;* large conductance $Ca^{2+}$- and voltage-activated $K^+$ channel (BK); white adipose tissue (WAT), brown adipose tissue (BAT); epididymal WAT (eWAT); interscapular WAT (intWAT); interscapular BAT (intBAT); mesenteric WAT (mesWAT); subcutaneous inguinal WAT (iWAT); 3T3-L1 cells*;* pre-adipocytes (pre-adipo); hormone-sensitive lipase (HSL); interleukin-6 (IL-6); leptin; adiponectin (ADIPOQ); browning; uncoupling protein 1 (UCP1)

**Number of words:** 4766 (max. 4000) (excluding title page, abstract, research design and methods**,** acknowledgments, references, and table/figure legends)

**Number of words (abstract):** 256 (max. 200)

**Number of references:** 61 (max. 50)

**Page count:** 31

**Abstract**

Elevated adipose tissue expression of the $Ca^{2+}$- and voltage-activated $K^+$ (BK) channel was identified in morbidly obese men carrying a *BK* gene variant supporting the hypothesis that $K^+$ channels affect metabolic responses of fat cells to nutrients. To establish the role of endogenous BKs for fat cell maturation, storage of excess dietary fat and body-weight (BW) gain we studied a gene-targeted mouse model with a global ablation of the *BK* channel ($BK^{L1/L1}$) and adipocyte-specific *BK*-deficient ($adipoqBK^{L1/L2}$) mice. Global *BK* deficiency afforded protection from high-fat-diet (HFD) induced BW gain and excessive fat accumulation. Expansion of white adipose tissue-derived epididymal $BK^{L1/L1}$ pre-adipocytes and their differentiation to lipid-filled mature adipocytes *in vitro*, however, were improved. Moreover, BW gain and total fat masses of usually super-obese *ob/ob* mice were significantly attenuated in the absence of *BK* together supporting a central or peripheral role for BKs in the regulatory system that controls adipose tissue and weight. Accordingly, HFD-fed $adipoqBK^{L1/L2}$ mutants presented with a reduced total BW and overall body fat mass, smaller adipocytes and reduced leptin levels. Protection from pathologic weight gain in the absence of adipocyte BKs was beneficial for glucose handling and related to an increase in body core temperature due to higher levels of uncoupling protein 1 as well as low abundance of the pro-inflammatory interleukin-6 as a common risk factor for diabetes and metabolic abnormalities. This suggests that adipocyte BK activity is at least partially responsible for excessive BW gain under high-caloric conditions suggesting BK channels as promising drug targets for pharmacotherapy of metabolic disorders and obesity.

**Introduction**

Obesity is caused by high calorie intake, typically derived from dietary fats or sugars. Over time, an imbalance between nutrient consumption and burning of calories leads to a massive increase in fat mass, which among other factors is a major cause of insulin resistance and diabetes (1; 2). Additionally, genetic mutations may cause excessive lipid accumulation and thereby a morbid gain in body weight (BW) emphasizing the multifactorial etiology of chronic excessive weight gain (3; 4). It has become increasingly clear that a variety of $K^+$ ion channels *i.e.* $K^+$ channels expressed within the brain and in the periphery, possibly by complex effects on appetite and satiety, energy expenditure, glucose balance and/or fat cell function, are involved in the patho-physiology of obesity and related disorders (5). Accordingly, a genome wide association study recently identified the human *KCNMA1* gene, encoding for the pore forming subunit of the large-conductance $Ca^{2+}$-activated $K^+$ channel (BK), as a novel susceptibility locus for obesity (6). *BK* channel mRNA levels in variant-carriers were significantly increased in white adipose tissue (WAT) and adipose tissue-derived cells, suggesting a pathogenic role for fat cell BK on metabolism. Others reported electrophysiological evidence for BK channels in human pre-adipocytes and BK knock-down, or its pharmacological inhibition, further revealed a possible link between channel activity and proliferative capacity of these cells (7), whereas $Ca^{2+}$-activated $K^+$ channels of the IK type seem to be dominant in the widely-studied murine pre-adipocyte model 3T3-L1 (8). Because both peripheral and central organs, involved in the control of metabolism, express BK it is, however, difficult to estimate the impact of pre-adipocyte BKs on fat cell formation and adiposity *in vivo*. For example, a direct modulation of BK by fatty acids and their metabolites seems to provide a possible link between lipid-mediated effects on the channel and altered vascular functions in hypertriglyceridemia secondary to obesity (9-13). Previous analyses of global *BK* knock-out mice imply that both glucose-induced insulin secretion and endocrine output from the hypothalamic-pituitary-adrenal (HPA) axis, require endogenous BK channels (14; 15). However, it has not been determined whether these dysregulations in β-cell or HPA function caused metabolic abnormalities *in vivo* (16). Moreover, several studies find BK promote inhibitory effects of leptin signaling, *via* PI3-kinase in hippocampal neurons (17) and in mouse chromaffin cells (18), suggesting that neuronal circuits controlling appetite and energy expenditure may also depend on functional BK. A malfunction of neuronal circuits has been widely appreciated as causing excessive fat storage (19) and a number of studies, indeed, found evidence for BK in brainstem, different hypothalamic nuclei, parts of

the cortex and limbic system, hence in brain regions that are implicated in the central control of food intake, appetite and energy expenditure (20; 21).

The recent discovery of functional channels with properties similar to BK in fat cell progenitors (7) together with the link between high fat cell *BK* mRNA expression levels and morbid adiposity (6) suggest that BK activity in the adipose tissue plays, yet to be discovered, physiologically and pathophysiologically important roles for weight control. In order to establish endogenous BK channels as potential modulators of fat deposition and excessive weight gain we herein assessed the susceptibility of global and adipocyte-specific *BK* mouse mutants towards genetic- and dietary-induced causes of adiposity. Our approach to validate BK as a novel player in the response to obesogenic factors *in vivo* should also direct future studies on the pharmacotherapy of adiposity and related disorders.

**Research design and methods**

**Animals and diets.** All animal experiments were performed with permission of the local authorities and conducted in accordance with the German legislation on the protection of animals. Animals were housed in cages under controlled environmental conditions with temperatures maintained between 21-24°C, humidity at 45-55% and 12h light-dark-cycle.

Global *BK* channel deficient mice (genotype: $BK^{L1/L1}$), heterozygous (genotype: $BK^{L1/+}$) and wildtype littermates (genotype: $BK^{+/+}$) on a C57BL/6N background were generated and maintained at the Institute of Pharmacy, Department of Pharmacology, Toxicology and Clinical Pharmacy, University of Tübingen as described previously (22). To produce $BK^{L1/L1}$ mice which are also unable to produce functional leptin (genotype: $BK^{L1/L1}$; $B6.V\text{-}Lep^{ob/ob}$ ($BK^{L1/L1}$; *ob/ob*)) $BK^{L1/+}$ animals were crossed to mice carrying a heterozygous mutation of the leptin-gene $B6.V\text{-}Lep^{+/ob}$ *J* (*ob*/+) obtained from Charles River, Germany. Intercrossing of double-heterozygous animals (genotype: $BK^{L1/+}$; $B6.V\text{-}Lep^{ob/+}$ ($BK^{L1/+}$; *ob*/+)) produced homozygous obese $BK^{L1/L1}$; *ob/ob,* obese $BK^{+/+}$ (genotype: $BK^{+/+}$; $B6.V\text{-}Lep^{ob/ob}$ ($BK^{+/+}$; *ob/ob*)), lean $BK^{L1/L1}$ ($BK^{L1/L1}$; $B6.V\text{-}Lep^{+/+}$ ($BK^{L1/\ L1}$; +/+)) and lean $BK^{+/+}$ ($BK^{+/+}$; $B6.V\text{-}Lep^{+/+}$ ($BK^{+/+}$; +/+)) offspring from the same litters. In order to obtain tissue-specific mutants lacking *BK* in various adipocyte populations heterozygous *BK* mice ($BK^{L1/+}$) on C57BL6 background, carrying a tamoxifen inducible adipose tissue-specific Cre recombinase (genotype: *adiponectin-CreERT2*$^{tg/+}$) under control of the adiponectin promoter (23), were first mated to homozygous floxed *BK* animals (genotype: $BK^{L2/L2}$). Adipocyte-specific controls (genotype: *adiponectin-CreERT2*$^{tg/+}$; $BK^{+/L2}$ (*adipoqBK*$^{+/L2}$)) and pre-mutant BK animals (genotype: *adiponectin-CreERT2*$^{tg/+}$; $BK^{L1/L2}$ (*adipoqBK*$^{L1/L2}$)) derived from this breeding were injected with tamoxifen (1 mg/d) for 5 consecutive days to induce Cre-mediated recombination at an age of 8 weeks (Fig. 3 and Fig. 4C-H) or 19 weeks (Fig. 4I).

The specificity and efficiency of the *adiponectin-CreERT2*-derived recombination was supported by studying double fluorescent ROSA26-Tomato reporter mice (genotype: $ROSA26^{mTomato/mEGFP}$ ((*tom*/+)) obtained from Charles River, Germany (24) expressing the adipoqCreERT2 transgene (genotype: *adiponectin-CreERT2*$^{tg/+}$; *ROSA26-Tomato*$^{tom/+}$; (*adipoq*$^{tg/+}$; *tom*/+). Double-transgenic animals were either injected with tamoxifen for 5 days as described to induce recombination of the reporter allele *i.e.* a switch from cell membrane-localized red fluorescence to green fluorescence proteins or received solvent. Genotyping was performed using specific primers to identify the Cre transgene (23), the single nucleotide mutation in the leptin gene (according to a protocol for Stock Number: 000632 by The Jackson Laboratory) and the L1, L2 and wild-type alleles of the BK on DNA samples

obtained either from different fat depots, control tissue or tail-tip biopsies from mice that were left untreated or received tamoxifen as described previously (22).

Prior to the different research diets, all experimental mice received tap water and a commercial chow obtained from Altromin, Germany ad libitum. Dietary feeding trials were performed in male mice that were allowed to adapt to a defined control-diet (CD) formulation containing 10% of calories due to fat for two weeks prior the long-term feeding experiments. With 10 weeks of age experimental mice either received a high-fat-diet (HFD) containing 45% or 60% of calories due to fat or were continued to feed the CD for another 18 weeks. Progressive body weight gain in the monogenetic model of obesity was monitored between 4 and 24 weeks of age on normal chow diet.

**Food intake and body core temperature measurements**

The core body temperature and the locomotor activity were measured by using a telemetry setup (ETA-F10 with the two-lead ECG transmitters of the implant removed because they were not required for monitoring the activity and temperature; Data Sciences, Inc.). The surgical procedure was described previously (25). In brief, anesthesia was induced by a 4% isoflurane in oxygen inhalation and was then maintained with 1-2% isoflurane. By aseptic technique the implants were placed in the peritoneal cavity and the skin was closed with a 5/0 surgical silk. During recovery, mice were placed on a warming pad before they were returned to their home cages for at least 3 days before recordings were started. Activity and body core temperature were assessed continuously for 96 hours in experimental mice that had received the HFD diet for 18 weeks.

Food intake was measured using a non-automated and modified metabolic cage setup. To reduce the environmental stress in the feeding chamber of the metabolic cage mice housed individually were placed on paper bedding that was renewed daily. After two days of acclimatization food consumption was assessed for 4 days using an analytic balance. Foot pellets were replaced every 24 hours. The amount of food consumed by each individual mouse was determined by calculating the weight differences between the initial weight of the pellets and the final pellet weights 24 hours later. Food pieces dropped by the animals on the paper bedding were thoroughly collected and included in the final weight determination. Food intake was assessed in a subset of experimental mice prior the dietary feeding at an age of 10 weeks or after the CD or HFD feeding protocols.

**Growth and maturation of pre-adipocytes *in vitro*.** Pre-adipocytes derived from iWAT or eWAT of 10 week old $BK^{+/+}$ and $BK^{L1/L1}$ mice were isolated by an established collagenase liberation protocol (26). Upon 50 min of digestion in Collagenase type I/HEPES buffer at 37°C, $2x10^4$ or $5x10^4$ cells/cm² from iWAT or eWAT were plated in DMEM-Ham's F12 with 5% FCS, respectively. At 90-100% cell confluency maturation was induced by addition of induction medium containing insulin (170 nM), dexamethasone (1 µM), isobutylmethylxanthin (500 µM) and indomethacine (30 µM) to eWAT cultures. Differentiation of iWAT pre-adipocytes was stimulated by adding rosiglitazone (2.5 µM) and triiodothyronine (1 nM) to the eWAT induction medium. After 48h of induction the medium was exchanged by insulin (170 nM) containing medium in DMEM-Ham'sF12 with 10% FCS for another 48h, followed by maintenance medium (DMEM-Ham'sF12 with 10% FCS). Maintenance medium was changed every second day until cells were mature, usually 14 to 16 days after plating. Triglyceride-incorporation was detected by Oil-red-O (ORO) staining. ORO-content was quantified by photometry using the Implen-system at 518 nm. Digital images of the maturation process were acquired using AxioVision software version 4.8 (Carl *Zeiss, Jena, Germany).* Cell-growth and proliferation assays were analyzed in real-time using the xCELLigence impedance setup (OMNI life science, Bremen, Germany) during the first 60 hours upon plating in DMEM-Ham'sF12 with 5% FCS medium. Data was acquired and analyzed using the RTCA software version 1.2.1 (ACEA Biosciencis Inc.).

**Electrophysiological recordings.** The conventional whole-cell mode of patch clamp electrophysiology was used to analyse BK currents in undifferentiated and differentiated 3T3-L1 cells as well as from pre-adipocytes and induced matured adipocytes prepared from primary cultures of mouse eWAT. The pipette solution contained 140 mM KCl, 10 mM HEPES, 30 mM Glucose, 1 mM BAPTA, 2 mM MgCl and free calcium buffered to 0.5µM at pH 7.2. The standard bath (extracellular) solution contained (in mM): 140 mM NaCl 5 mM KCL 10 mM HEPES, 20 mM Glucose, 2 mM MgCl and 1 mM CaCl and pH was adjusted to 7.4. Electrophysiological recordings were performed at room temperature (18-22°C) using pCLAMP 9 (Molecular Devices) with a sampling rate of 10 kHz and filtered at 2 kHz. Patch pipettes were fabricated from borosilicate glass (Garner) with resistances between 2-3 MΩ. Drugs were applied to cells using a gravity perfusion system with a flow rate of 1-2 ml/min to minimise flow-induced artefacts. For analysis of BK currents, the BK channel specific blocker paxilline (1µM) was applied and the paxilline-sensitive outward current analysed at the membrane voltages indicated in the respective figure legends.

**Adipose tissue histology.** For histological examination tissues were fixed in 4% paraformaldehyde for 1.5 hours directly after harvesting and were then embedded in NEG 50™ (Richard-Allan Scientific, Thermo Scientific) for sectioning following sucrose-gradient cryoprotection. Serial 14-µm cryo-sections of different WAT depots were prepared using a HM 560 cryostat (Thermo Scientific, Waltham, USA) and stored at -80°C until further processing. To determine the size of the fat cells prior to and after different diets their perimeter was determined in digital images of the iWAT depot using the AxioVision software package version 4.8 (Carl *Zeiss, Oberkochen, Germany)*. The uncoupling protein 1 (UCP1) expression pattern was compared between iWAT cryo-sections obtained from HFD-fed *adipoqBK*$^{L1/L2}$ and *adipoqBK*$^{+/L2}$ mice using a commercial antibody (Santa Cruz, Dallas, USA) (dilution 1:400). BK immunodetection was performed in iWAT and eWAT sections derived from 10-week old global and adipocyte-specific BK mutants and control litters using a primary antibody, specific for the BK channel alpha subunit (dilution 1:1000) and hormone-sensitive lipase (HSL; dilution 1:400) according to a previously published protocol (27). In brief, antigen-antibody-complexes were detected by a fluorescense-labeled secondary antibody (AlexaFluor®568; anti-rabbit) (dilution 1:500) using the AxioCam MR system (Carl Zeiss, Oberkochen, Germany*)* or by appropriate secondary antibodies conjugated to horseradish peroxidase (dilution 1:500).

**Adipose tissue mass and total body composition.** To determine total fat mass and individual mass of different depots fat pads were dissected unfixed upon dietary-feeding then weighed, immediately immersed in liquid nitrogen and finally stored at -80°C for further analysis. For total body-composition analysis total body weight was determined prior and after drying the corpse for 24 hours at 85°C. Water content was calculated as difference between dry and total weight. Fat-content was determined in dried corpses using the Soxhlet procedure according to a previously published protocol (28).

**Blood parameters and glucose tolerance test.** Blood was collected from mice prior to or after dietary feeding. Leptin, IL-6 and adiponectin levels were measured in serum samples with mouse immunoassay kits (Merck Millipore, Darmstadt, Germany) according to manufacturer's instructions. Blood glucose was determined using the GlucoCheck advance system (TREND Pharma GmbH, Saalfeld/Saale, Germany) immediately before i.p. glucose challenge (2 g/kg of body-weight) as well as 15, 30, 60 and 120 min after the injection in

over-night fasted mice. At each time additional blood (25 µl) was collected via the tail vein for subsequent insulin determination. Plasma-Insulin was measured using the Ultra Sensitive mouse Insulin ELISA (Mercodia, Uppsala Sweden), according to manufacturer's instructions.

**mRNA expression analysis.** Total mRNA was extracted from WAT samples by a guanidineisothiocyanat-phenol-chloroform extraction protocol using PegGold RNA Pure (Peqlab Biotechnologie, Erlangen, Germany) according to the manufacturer's instructions. Following DNase treatment for 30 min to remove traces of genomic DNA, RNA samples were quantified and 0.5 µg RNA were used to generate cDNA using the ISRIPT cDNA synthesis kit (Bio-Rad, Hercules, USA). Quantitative real-time PCR was performed in triplicates using the comparative $2^{-\Delta C(t)}$ method, with C(t) indicating the cycle number at which the signal of the PCR product crosses the threshold, set within the exponential phase of the detected fluorescence signal. BK- and IL-6-levels were normalized to β-actin to determine their relative quantitates. The respective primer sequences designated were: BK forward: 5'-GAC GCC TCT TCA TGG TCT TC -3', BK reverse: 5'-TAG GAG CCC CCG TAT TTC TT-3'; IL-6 forward: 5'- CTT CAA CCA AGA GGT AAA AG -3', IL-6 reverse: 5'-CCA GCT TAT CTG TTA GGA GAG -3'. For extraction of total mRNA from 3T3-L1 cells or pre-adipocytes and differentiated adipocytes in culture the Roche High pure mRNA extraction kit was used according to the manufacturer's instructions following shearing of cells in lysis buffer using a 25G needle. Following DNase treatment as above 0.25 µg RNA were used to generate cDNA using the Roche Transcriptor Hi-Fidelity cDNA synthesis kit with random hexamers and oligo-dT used at a 2:1 ratio. qRT-PCR was performed using the comparative $2^{-\Delta\Delta C(t)}$ method as above with mRNA levels normalized to Ipo8. The respective primers were: BK forward: 5'-GTC TCC AAT GAA ATG TAC ACA GAA TAT C; BK reverse primer: 5'-CTA TCA TCA GGA GCT TAA GCT TCA CA; GLUT4 using the Quantitect Assay (Mm_Slc2a4_2_SG) and Ipo8 using Quantitect assay (Mm_Ipo8_2_SG) from Qiagen.

**3T3-L1 culture and differentiation.** Undifferentiated (UD) 3T3-L1 fibroblasts were maintained in Dulbecco's modified Eagle's Medium (DMEM) containing 10% fetal bovine serum (FBS) and 1% penicillin/streptomycin at 37°C at 10% $CO_2$ and passaged every 4 days after reaching 60-80% confluency. Differentiation was initiated in confluent monolayers in DMEM/FBS containing 1µg/ml insulin, 0.25µM dexamethasone, 1µM troglitazone and 500µM IBMX for 3 days followed DMEM/FBS containing 1µg/ml insulin and 1µM troglitazone. After 3 days cell medium was replaced with DMEM/FBS and medium refreshed

every 3 days until differentiated cells (DF) were analysed (typically 10-14 days after initiation of differentiation).

**Immunoblot analysis of iWAT and 3T3-L1 derived protein lysates.** Inguinal WAT was dissected and processed as described in order to generate total protein lysates for subsequent immunoblot analyses (27). Total protein was obtained from undifferentiated and differentiated 3T3-L1 fibroblasts. Separation of the proteins by molecular weight was done by gel electrophoresis using 12% SDS gels. For immunodetection primary UCP1 (Santa Cruz, Dallas, USA) (dilution 1:1000), Glyceraldehyde-3-phosphate dehydrogenase (GAPDH, dilution 1:1000) (Cell Signaling), glucose transporter type 4 (GLUT4, 1:1000) (generous Gift from Gwyn Gould, Glasgow, UK), BK (1:1000) (NeuroMab, UC Davis, USA) and β-actin (1:500) (Sigma-Aldrich, St. Louis, USA) antibodies were used.

**Statistical analysis.** Statistical analysis was performed on experimental data using a two-tailed student's t-test for paired or unpaired comparison or ANOVA with post-hoc Dunnett's test for multiple comparisons where appropriate. All data are presented as mean ± SEM. For all tests, p-values less than 0.05 were considered as significant: $P<0.05$ (*), $P<0.01$ (**), $P<0.001$ (***).

**Results**

Body weight (BW) gain was investigated in global BK-deficient ($BK^{L1/L1}$) and age- and litter-matched male wild-type mice ($BK^{+/+}$) (Fig. 1A) receiving either a purified low-fat control (CD) or a high-fat diet (HFD). Prior to the different diets we observed a small but highly significant ($P<0.001$) difference in the BWs between the two genotypes as previously reported (29; 30). Starting with 5 weeks of HFD feeding, however, a substantial weight gain in male $BK^{+/+}$ mice became apparent resulting in a total BW gain of 16.44 ± 0.83 g for $BK^{+/+}$ mice at the end of a 18 weeks HFD feeding protocol (Suppl. Fig. 1A), whereas $BK^{L1/L1}$ mutants gained 8.37 ± 0.45 g in the same observation period. Importantly, the differences in BW gain of $BK^{L1/L1}$ mutants were about than 10 % for CD (33.34 ± 2.38%) and HFD (44.26 ± 2.68%) fed groups, whereas the respective difference in the diet induced BW gain for $BK^{+/+}$ mice was 27.76% (Suppl. Fig. 1B). Neither daily food intake of $BK^{+/+}$ and $BK^{L1/L1}$ mice under CD- or HFD-fed conditions (Suppl. Fig. 1C) nor the activity or body-temperature of the animals differed significantly (Suppl. Fig. 1D-E) under HFD suggesting that the lean phenotype of the $BK^{L1/L1}$ mice was, at least not primarily, due to abnormal hyperactivity or dysfunctions in central control of peripheral circuits regulating food intake and reward behaviors. Body-composition revealed that the HFD feeding did not affect wet body mass and carcass dry mass but rather stimulated a substantial increase in the total body fat mass in $BK^{+/+}$ mice, whereas the respective body-composition of CD- and HFD-fed $BK^{L1/L1}$ did not differ (Fig. 1B) supporting the notion that the genotype-specific differences in BW upon CD and HFD feeding (Fig. 1A) are largely due to reduced accumulation of fat in the absence of *BK*. Less total body fat mass of CD- and HFD-fed $BK^{L1/L1}$ mice were accompanied by a small but significant shift to lower dry mass values and reduced tibial length (TL) (Suppl. Fig. 1F) both confirmatory for the lower overall body size in the global absence of BK channels (Fig. 1C). Analyses of fat mass-normalized to TL revealed significant weight differences for various white adipose tissue (WAT) depots as well as the interscapular brown adipose tissue (BAT) indicating that the lean phenotype of the $BK^{L1/L1}$ mice was related to a decrease in multiple adipocyte tissue cell populations (Fig. 1D). So far, the data suggest that high-caloric nutrition-induced BW gain requires functional BK channels. Additionally, the reduced TL, in the global *BK* knock-outs is in accordance with previous reports collectively implying a mild growth defect that may contribute, at least partly, to the differences observed between $BK^{+/+}$ and $BK^{L1/L1}$ BW during dietary feeding (30). We next tested whether BK plays a role for the excessive fat accumulation in the monogenic *ob/ob* model of morbid obesity. BW gain (Suppl. Fig. 2A), body-composition (Suppl. Fig. 2B+C) and individual weights of different fat

depots (Suppl. Fig. 2D) were studied in *BK*-negative *ob/ob* double-mutants and age- and litter-matched *ob/ob* controls. In line with the HFD-fed $BK^{+/+}$ and $BK^{L1/L1}$ mice we find that key parameters of the progressively developing super-obese phenotype, including body weight, body-composition and fat depot masses are attenuated in the absence of BK (Suppl. Fig. 2A-D). In contrast, differences in BW gain between lean control mice in the absence ($\Delta$16.83 ± 0.55 g) and presence ($\Delta$15.73 ± 0.55 g) of BK were not significant ($p = 0.17$). Protection against overwhelming BW gain in the *BK*-deficient *ob/ob* model was related to a consistent effect on total fat masses and non-fat components of the body (Suppl. Fig. 2B). Indeed, a lower initial as well final BW of BK-negative lean and *ob/ob* double-mutant mice (Suppl. Fig. 2A) as well as differences in the mean TL (Suppl. Fig. 2E) suggest that BK plays a role for normal growth development (Suppl. Fig. 2) and morbid obesity resulting from leptin deficiency.

Based on previous reports on the role of $K^+$-channels in adipocytes (6; 7) and our consistent observation of lower fat masses of multiple fat depots (Fig. 1D and Suppl. Fig. 2D) we considered that the protection from overwhelming weight gain was stemming from the adipocyte itself. To address this possibility, we first assessed the *BK* mRNA and protein expression in inguinal and epididymal white adipose tissue (iWAT and eWAT, respectively). Fat pads were studied using primer pairs allowing for specific detection and quantification of *BK* mRNA (Fig. 1E+F). As compared to the internal reference *BK* levels in $BK^{+/+}$ iWAT and eWAT depots were low but reliable amplification was accomplished in all samples tested. Importantly, signal traces detected in the respective fat depots derived from $BK^{L1/L1}$ mice were well in the range of non-specific PCR product formation in the absence of reverse transcriptase (Suppl. Fig. 3A+B). Because adipose tissue is heterogeneous, composed of fat- and non-fat cells, we next examined the cellular distribution of BK channel protein in frozen adipose tissue sections obtained from 10 week old $BK^{+/+}$ and $BK^{L1/L1}$ mice. These analyses revealed evidence for BK in unilocular $BK^{+/+}$ cells, characteristic of white adipocytes, whereas $BK^{L1/L1}$ iWAT and eWAT remained BK-negative (Fig. 1G+H). Importantly, our specific BK antibodies and an antibody for the white fat cell marker hormone-sensitive lipase (HSL) marked the same cells in $BK^{+/+}$ eWAT (Suppl. Fig. 3C) supporting the notion that mature adipocytes express BK channels.

To explore the functional attributes of endogenous BK channels in adipocytes we adopted a previously established protocol of primary culture and differentiation of murine adipocyte

precursor cells (26). Adipocyte differentiation was induced at 90-100% confluence of $BK^{+/+}$ and $BK^{L1/L1}$ precursor cells derived either from eWAT and iWAT depots. Oil-red-O (ORO) incorporation into lipid droplets revealed strong accumulation of lipid-filled adipocyte-like cells under adipogenic maintenance conditions in cell cultures derived from both *BK*-negative and $BK^{+/+}$ eWAT (Fig. 2A-C) and iWAT (Fig. 2D-F). In iWAT-derived cultures we did not observe differences in the adipogenic differentiation among genotypes (Fig. 2D-F), whereas the amount of ORO incorporation was significantly higher in $BK^{L1/L1}$ than $BK^{+/+}$ cultures established from eWAT (Fig. 2A-C) suggesting a depot-specific role for BK on *in vitro* lipid-storage. Moreover, genetic and pharmacological blockade of BK channels enhanced the growth of eWAT-derived pre-adipocytes (Fig. 2G+H).

To further validate differentiated adipocytes from eWAT express functional BK channels, we assayed BK mRNA, protein and ionic currents in the differentiated cultures. BK channel, as well as GLUT4 transporter, mRNA and protein were strongly upregulated in differentiated cells compared to precursor cells (Fig. 2I+J). Importantly, outward potassium currents, sensitive to the specific BK channel blocker paxilline (1 μM), were significantly upregulated in differentiated adipocytes (Fig. 2K). An increase in BK channel mRNA, protein and currents were also observed in the established 3T3-L1 pre-adipocyte cell model following induction of differentiation (Suppl. Fig. 4A-C). In addition, inhibition of BK channels with paxilline increased the growth of 3T3-L1 pre-adipocytes and the amount of ORO incorporation into lipid droplets (Suppl. Fig. 4D+E). Taken together, these data suggest that fat cell BK channels control pre-adipocyte expansion and adipogenic conversion of pre-adipocytes in an adipocyte depot specific manner.

Because homeostasis of mature adipocyte and adipocyte differentiation *in vivo* are distinct from the above studied *in vitro* models, we next studied the lean phenotype by generating an adipocyte-specific BK knock-out mouse model ($adipoqBK^{L1/L2}$). In a first series of experiments we confirmed the tissue-specific recombination efficacy of the recently established adiponectin promotor-driven tamoxifen-inducible CreERT2 mouse model (23) using a two-color fluorescent Cre reporter system (24). Prior to Cre-mediated excision we observed ubiquitous expression of a cell membrane-targeted red fluorescent Tomato (mT) in eWAT, iWAT and all other tissues studied suggesting that the $ROSA^{mT/mG}$ mouse is indeed a global Cre reporter model (Fig. 3A+B and data not shown). Tamoxifen induced Cre-mediated excision of the floxed *mT* was leading to an almost complete switch to green fluorescent protein (mG) expression in eWAT and iWAT fat cells, whereas changes in mT labelling were not observed in various other organs such as brain, skeletal muscle, and liver (data not

shown). High efficiency and specificity of the adiponectin-CreERT2 approach was further confirmed by a *BK* specific primer set designed to identify the three different *BK* alleles *i.e.* wild-type (+), floxed (L2) and knock-out (L1) within one sample. In line with the Cre-reporter assay (Fig. 3A+B) PCR products indicative of a recombination event were only observed in white and brown adipocyte tissues of adiponectin-CreERT2 transgenic $BK^{+/L2}$ mice ($adipoqBK^{+/L2}$), whereas analysis of multiple other cell types and organ systems did not reveal significant Cre activity regardless of whether tamoxifen was applied or not (Fig. 3C). As compared to $adipoqBK^{+/L2}$ controls, eWAT and iWAT *BK* mRNA expression levels were reduced in tissue-specific $adipoqBK^{L1/L2}$ mutants upon tamoxifen application (Fig. 3D). Accordingly, adiponectin-CreERT2 activation by tamoxifen resulted in a nearly complete ablation of the BK protein in the different WAT tissues (Fig. 3E+F). Hence, the adipocyte-specific knock-out model of *BK* should allow us to test the role of fat cell BK channels for BW gain under CD- and HFD-feeding conditions in the absence of changes in satiety or adiposity signals arising from endocrine or neuronal circuits potentially involving hypothalamic BK channels among others. To induce site-specific recombination of the L2 *BK* gene locus, $adipoqBK^{L1/L2}$ mice as well as $adipoqBK^{+/L2}$ control age- and littermates were subjected to the tamoxifen injection 2 weeks prior to the experimental diets *i.e.* a CD or a HFD with 60% of its calories derived from fat (Fig. 4A+B). Consistent with our previous findings in the global $BK^{L1/L1}$ model (Suppl. Fig. 1C), the tissue-specific ablation of BK did not affect the amount of CD or HFD food consumed by the animals at the start or end of the feeding experiment (Fig.4C+D). Starting BWs and BW gain in the CD group were not different between $adipoqBK^{+/L2}$ and $adipoqBK^{L1/L2}$ mice (Fig. 4E+G), whereas lack of adipocyte BK channels afforded partial protection against HFD-induced gain in BW (Fig. 4F+H), an effect that reached the significance level after 4 weeks of HFD-feeding and was maintained until the mice reached their final BWs (Fig. 4F) indicative for a lower susceptibility of $adipoqBK^{L1/L2}$ mutant mice towards high caloric challenges. We next tested whether excess BW gain is also affected by fat cell BK in mice which have already established significant weight gain. To test this, tamoxifen treatment was commenced at an age of 19 weeks when the $adipoqBK^{+/L2}$ control and $adipoqBK^{L1/L2}$ pre- mutants had reached a BW of 32.35 ± 1.05 g and 31.91 ± 0.89 g, respectively. Total BW gain was not different between age-and litter-matched $adipoqBK^{+/L2}$ and $adipoqBK^{L1/L2}$ mice prior to the tamoxifen treatment ($t_{10\text{-}19}$ 8.18 ± 1.00 g for $adipoqBK^{+/L2}$ and $t_{10\text{-}19}$ 7.71 ± 0.76 g for $adipoqBK^{L1/L2}$ (P = 0.7)), whereas upon five repetitive tamoxifen injections the extent of the weight gain showed

a clear tendency towards lower values in *adipoqBK*$^{L1/L2}$ mice (Fig. 4I) ($t_{20\text{-}30}$ 5.33 ± 0.56 g for *adipoqBK*$^{L1/L2}$ and $t_{20\text{-}30}$ 7.40 ± 1.03 g for *adipoqBK*$^{+/L2}$ (P<0.06))

In depth analyses of the individual fat depots (Fig. 5A+G) and the total fat mass (Fig. 5B) did not reveal statistical weight differences between *adipoqBK*$^{+/L2}$ and *adipoqBK*$^{L1/L2}$ fed a CD diet. HFD feeding, however, confirmed protection from excessive fat storage in *adipoBK*$^{L1/L2}$ mice. Interestingly, lack of adipocyte BK was associated with lower total fat masses and lower masses of various fat depots (Fig. 5C-G). Because fat mass is determined by both adipocyte number and size we next studied fat storage at the cellular level. Inguinal WAT cell size was calculated by assessing the cell perimeters in different cryo-sectional areas obtained from *adipoqBK*$^{+/L2}$ and *adipoqBK*$^{L1/L2}$ mice. Prior to the different diets *i.e.* at an age of 10 weeks genotype-specific differences in fat cell size were not detectable in different areas of the iWAT sections (Fig. 6A+C). As compared to *adipoqBK*$^{+/L2}$ fat cells, *BK*-deficient adipocytes were smaller upon CD and HFD feeding (Fig. 6A+C). Because enlarged, hypertrophic fat cells in the adipose depot relate to obesity, inflammation and insulin resistance we next tested whether the observed changes in adipocyte morphology (Fig. 6A-C) associates with a more proinflammatory state. Indeed, we find reduced IL-6 mRNA expression in iWAT of HFD-fed *adipoqBK*$^{L1/L2}$ mice and tendentially lower serum IL-6 levels (Fig. 6E; p = 0.11). Moreover, HFD-fed *adipoqBK*$^{L1/L2}$ mice exhibited lower serum leptin levels as a marker of body-mass (Fig. 6F), whereas adiponectin concentrations were not different between diets or genotypes (Fig. 6G). In accordance with the markers of inflammation, low adipose tissue mass and fat cell hypertrophy, *adipoqBK*$^{L1/L2}$ mice showed an improved glucose clearance (Fig. 6H) with lower insulin levels (Fig. 6J) upon intra-peritoneal glucose challenge after HFD-feeding, whereas lack of adipocyte BK did not affect glucose handling prior to the feeding protocol (Fig. 6I). Change in cellularity of the iWAT may also be taken as an indicator for accelerated browning to promote energy expenditure which will counter obesity and its metabolic consequences. Lack of fat cell BK resulted in strong induction of the uncoupling protein 1 (UCP1) (Fig. 7A+C) as a hallmark of uncoupled respiration and heat production by brown or brown adipocyte-like fat cells. Higher levels of UCP1 protein under HFD-fed conditions were also reflected by a significant increase in core body temperature during the night (Fig. 7D), whereas during the day, while the mice were sleeping, body temperatures of *adipoqBK*$^{L1/L2}$ and *adipoqBK*$^{+/L2}$ mice were lower suggesting a reduced burning of stored fats with no apparent differences between the two genotypes (Fig. 7D).

In summary, adipocyte BKs promote fat cell size and fat pad mass *in vivo.* Adipocyte tissue growth in the presence of endogenous BK channels was related to a noninfectious activation of adipose tissue inflammation and metabolically unfavourable effects on fat cell functions, which together may result in insulin resistance and amplified HFD-induced adiposity.

**Discussion**

By combined analysis of different BK channel mutant mouse lines we have uncovered a novel function for adipocyte BKs in fat cell biology and metabolism under different nutritional conditions. We find resistance to HFD-induced BW gain, lower total fat mass and thereby improved glucose handling upon ablation of endogenous BK channels in adipose depots in different parts of the body. These data imply that the development of obesity caused by nutrient excess is promoted by the BK channel (Fig. 4). Accordingly, a previously identified *BK* gene variant was associated with elevated levels of fat cell BK mRNA in morbidly obese human subjects suggesting a causal relationship between the amount of adipocyte BKs and weight gain (6). To the best of our knowledge, BK levels in other organ systems of the affected patients have not been assessed; therefore, it remains unclear if the obesogenic effects attributed to amplified BK expression resulted exclusively from an effect on adipocyte cell function or whether BK channels present in non-adipocyte cells contributed to morbid weight gain. Interestingly, our HFD-fed $BK^{L1/L1}$ mutants did not exhibit any changes in dietary food consumption or body temperature (Suppl. Fig. 1C+D), whereas the respective fat-cell specific mutants exhibited a lean phenotype that was related to an increase in UCP1 levels and energy expenditure (Fig. 7). It therefore seems tempting to speculate that BK channels in the brain or other non-fat cells dot no play a role for the chemical and neural signals regulating calorie intake and/or energy expenditure and thereby body composition. For several reasons, however, we find it is too early to draw such conclusions:

*i.*) Our previous analyses of the global $BK^{L1/L1}$ mouse model revealed multiple defects in various systems of these animals including in β-cells (15), the HPA-axis (14) and cerebellar neurons (29), which separately or together could affect energy balance and BW development. For example, lack of cerebellar BK channels in Purkinje cells, among other deficits, was shown to cause motor learning impairment and signs of ataxia with the latter being related to muscle shivering and trembling (29), a common cause for increased energy expenditure. Irrespective of the dietary fat content we did not observe an increase in the body core temperatures of $BK^{L1/L1}$ mice (Suppl. Fig. 1D) suggesting that their very low body-fat content (Fig. 1) allow them to keep body temperature at physiological levels. Potential changes in body temperature regulation *i.e.* adjustments due to changes in non-/shivering thermogenesis may be superimposed by the loss of heat in $BK^{L1/L1}$ mutants. Yet, $BK^{L1/L1}$ mice present with a lean phenotype with CD and HFD feeding regimes and we observed a lower propensity of the *BK/ob* double mutants to accumulate excessive body weight and fat mass. This suggests that the global lack of BK channels for the entire lifespan prevents the excessive BW gain, an

effect that was more obvious in the presence of genetic or nutritional risk factors for obesity development. In this complex mouse model, a dysregulation of multiple pathways (in fat cells, hypothalamus, liver, sympathetic neurons, β-cells, etc.) involving BK may be related to this phenotype.

*ii.)* The protection in terms of BW gain and fat accumulation was less pronounced in adipocyte specific BK knock-out groups as compared to the $BK^{L1/L1}$ or *BK/ob* double mutant models (compare Fig. 1A, Suppl. Fig. 2A and Fig. 4F) implying non-fat cell BKs are also important for weight control *in vivo.* Indeed, dietary-related changes in energy expenditure involving, for example, hypothalamic control mechanisms may be positively or opposingly regulated by BK channels of neuronal nuclei that respond to satiety or hunger signals. Lack of GIRK4, a G protein-gated inwardly rectifying $K^+$-channel, in mice, for instance, resulted in late onset obesity through hypothalamic mechanisms (31), whereas ATP-sensitive $K^+$ channel ($K_{ATP}$) knock-out mice showed hyperphagia but were resistant to HFD induced BW and visceral fat mass gain (32). Along these lines, $K_{ATP}$ conductance in diet-induced obesity has been reported in pro-opiomelanocortin positive nuclei of the hypothalamus, and neuronal excitability and thereby the release of peptides that control food intake and BW were sensitive to central $K_{ATP}$ inhibition (33). In addition to $K_{ATP,}$ BK channels have been shown to modulate the excitability of hypothalamic neurons in response of insulin and leptin under physiological conditions (34) suggesting they may be involved in central circuits regulating BW *via* energy intake and expenditure. Given the complexity of the different metabolic pathways future studies are needed to clarify the functional roles of hypothalamic and other non-fat cell BK channels in adiposity and thereby the mechanism(s) underlying the lean phenotype of $BK^{L1/L1}$ mice. Resistance to genetic and diet-induced models of obesity *i.e.* hypothalamic-driven obesity has also been reported in mice with a Shaker family voltage-dependent $K^+$ channel gene disruption in *Kv1.3* (35; 36), further highlighting the importance of $K^+$ channels for the hypothalamic-regulation of BW (37). More recently, however, therapeutic benefits on obesity and insulin resistance upon Kv1.3 inhibition by using a blocker which was unable to cross the blood–brain barrier have been attributed to peripheral mechanisms stemming from changes in liver and WAT metabolism and brown adipose tissue (38). Obviously, peripheral and central $K^+$-channels affect the development of adiposity.

Studying adipocyte-specific *BK* knockout mice, we did not find any evidence for tamoxifen-induced recombination in different brain regions including the hypothalamus and other tissues involved in total body metabolism such as muscle or liver (Fig. 3) suggesting that partial protection from diet-induced obesity (Fig. 4F) is resulting from the lack of BK channels in

adipocytes (Fig. 3). Further, we observed amplified BK expression and currents with adipogenic differentiation of both mouse adipocytes from eWAT fat cell precursors as well as in the pre-adipocyte 3T3-L1 cell line (Fig. 2K and Suppl. Fig. 4C). Pharmacological blockade of BK channels stimulated both growth and lipid incorporation supporting a role of BK channels as regulators of cell cycle progression in human pre-adipocytes (7). By assessing BK-deficient eWAT and iWAT derived pre-adipocytes *in vitro*, however, we recognized fat depot specific functions for endogenous BK channels potentially involved in control of cell growth and lipid accumulation (Fig. 2). Because adiposity is usually induced through hypertrophic expansion of existing adipocytes leading to dysfunctional cells, an increase in the number of fat cells *i.e.* hyperplasia is proposed as mechanism that preserves metabolic fitness (39). Accordingly, lower levels of the pro-inflammatory cytokine IL-6 (Fig. 6D+E), significantly lower body weight (Fig. 4F), and smaller iWAT cell size together support the notion that lack of BK leads to the production of more "healthy" adipocytes that may afford protection against excessive BW gain thereby maintaining a regular response to the action of insulin. Reportedly, adipocytes produce and release IL-6 (40). In obesity the fraction of adipose-tissue derived IL-6 may promote a chronic state of low-grade inflammation affecting metabolism and development of insulin resistance (41). In comparison to $adipoqBK^{L1/L2}$ mutant mice we find higher IL-6 adipose tissue mRNA ($p < 0.05$) and non-significantly elevated serum levels ($p = 0.11$) in HFD-fed $adipoqBK^{+/L2}$ control mice, hence, it appears that fat cell BK channel activity is positively related to the adipose tissue IL-6 pathway providing a link between BK and obesity-related co-morbidities such insulin resistance (Fig. 6D+E and H). Interestingly, high plasma and adipose tissue levels of IL-6 were previously reported for the *ob/ob* mouse model (42), suggesting that BK channels may interfere with both, the genetic- and dietary-induced causes of adiposity by an IL-6-dependent mode of action. Along the same lines, HFD over-nutrition of $adipoqBK^{L1/L2}$ mice revealed lower total fat mass and smaller fat cells in iWAT depots. Of note, iWAT cells and depots differed in size and mass only *in vivo* (Fig. 6), whereas in pre-/adipocyte cultures originating from iWAT pads we did not detect differences in terms of various adipogenic parameters (Fig. 2). The reason for this apparent discrepancy is unclear although several mechanisms could be involved. First, *in vivo* the adipocyte-specific lack of BK channels results in a decrease of the iWAT but not eWAT depot fat mass. A "normal" mass of the $adipoqBK^{L1/L2}$ eWAT depot *in vivo* (Fig. 5A+C) may result from direct effects of the BK on the lipid storage and cell growth capacities and both parameters were augmented in the respective $BK^{L1/L1}$-derived fat cells *in vitro* (Fig. 2A-C and G+H). In contrast, a lower eWAT depot mass in the global BK knockouts (Fig. 1D) may

result from dysregulation of BK-dependent mechanisms in non-adipocytes. Interestingly, our observations in HFD-fed *adipoqBK*$^{L1/L2}$ and *adipoqBK*$^{+/L2}$ mice imply a small but significant increase of approx. 0.3°C in the body's core temperature in the absence of fat cell BKs (Fig. 7D), which indicates that these channels are involved in the thermogenic program of adipose cells. Presence of UCP1 in iWAT is characteristic of a process known as browning where this depot acquires brown adipocyte-like catabolic functions (43), and we find the adipocyte-specific ablation of BK channels to result in elevated mRNA (data not shown) and protein levels of iWAT UCP1 (Fig. 7A-C). Burning of stored fats by expansion or activation of BAT or by browning of WAT may result in a metabolically favorable phenotype (44). Accordingly, we observed a large fraction of smaller fat cells in iWAT, lower iWAT and total fat depot weights as well as an improved glucose homeostasis and insulin sensitivity in HFD-fed *adipoqBK*$^{L1/L2}$ mice (Fig. 7A-C and H-J).

Clearly, the mechanistic details underlying the lean phenotype of HFD-fed *adipoqBK*$^{L1/L2}$ mutants require future investigation. In general, it is widely accepted that BK channels are activated either by a raise in intracellular $Ca^{2+}$ ($[Ca^{2+}]_i$) or by membrane depolarization. $[Ca^{2+}]_i$ dynamics have a multifaceted role for brown adipocyte-like functions and for the formation of mature fat laden adipocytes (45-52), however relatively little is known about $Ca^{2+}$ signaling in white and brown adipocytes despite its suggested importance (53). Yet, efflux of $K^+$ *via* BK in non-excitable cells such as adipocytes may serve as a positive regulator for $Ca^{2+}$-entry as well as a number of $Ca^{2+}$-dependent processes, whereas in excitable cells BK is usually part of a negative feedback loop limiting influx of $Ca^{2+}$ via voltage-dependent $Ca^{2+}$ channels (54). Recently, transient receptor potential vanilloid 4 (TRPV4) channels have been identified as a major feature of the influx of extracellular $Ca^{2+}$ into fat cells (55). TRPV4 appears to negatively regulate the thermogenic and proinflammatory programs in adipocytes and mice with a TRPV4 ablation were protected from diet-induced obesity, hence TRPV4 deficiency results in a phenotype very similar to that caused by adipocyte-specific BK ablation. A functional coupling of BK and TRPV4 was reported in different systems (56; 57). Although this paper did not examine this link, we hypothesize that BK may suppress the acquisition of brown adipocyte-like features in white fat cells by an effect on the $Ca^{2+}$-entry and subsequent signaling pathways involving TRPV4 or other $Ca^{2+}$-permeable members of the large TRP channel protein family (50; 51; 58).

Finally, BK channels are common targets of various intracellular signaling molecules including cyclic guanosine-3′,5′-monophosphate (cGMP) and cyclic adenosine-3′,5′-monophosphate (cAMP) (59; 60). It is well established that both, cAMP and cGMP pathways,

play, among others processes, differential roles in lipolysis, browning of WAT and brown fat cell thermogenesis (44; 61), which should allow for complex adjustments of BK function in the different fat depots *in vivo* under patho-/physiological conditions.

Together, the presented data show that loss of fat cell BK channels supports the browning of fat cells to enhance thermogenesis in response to nutritional excess thereby limiting excessive weight gain. Targeting fat cells with BK channel inhibitors may thus hold potential to reduce pathologic features of excessive weight gain and related disorders.

**Acknowledgments**

The authors thank Clement Kabagema-Bilan, Isolde Breuning, Michael Glaser, and Katrin Junger (all from the Department of Pharmacology, Toxicology and Clinical Pharmacy, Institute of Pharmacy, University of Tuebingen, Tuebingen, Germany) for excellent technical help.

**Funding**

The work was in part funded by: The Deutsche Forschungsgemeinschaft (to RL and PR), the Wellcome Trust (to MJS and PR), and Diabetes UK (to MJS and LHC).

**Duality of interest**

No potential conflicts of interest relevant to this study were reported.

**Author Contributions**

*Research design:* PR, MJS, and RL; *conducted experiments:* JI, LT, HM, MW, and MJS; *contributed new reagents, techniques or analytic tools:* LHC, VL, AS, and SO; *data analysis:* JI, MJS, and RL; *wrote or contributed to the writing of the manuscript:* JI, MJS, and RL; *Contributed to discussions*: PR; *approved the final manuscript: all authors.* RL *and* MJS *are the guarantors of this work and, as such, take responsibility for the integrity of the data and the accuracy of the data analysis.*

**References**

1. Gesta S, Tseng YH, Kahn CR: Developmental origin of fat: tracking obesity to its source. Cell 2007;131:242-256
2. Kahn SE, Hull RL, Utzschneider KM: Mechanisms linking obesity to insulin resistance and type 2 diabetes. Nature 2006;444:840-846
3. Choquet H, Meyre D: Genetics of Obesity: What have we Learned? Current genomics 2011;12:169-179
4. Ramachandrappa S, Farooqi IS: Genetic approaches to understanding human obesity. The Journal of clinical investigation 2011;121:2080-2086
5. Sohn JW: Ion channels in the central regulation of energy and glucose homeostasis. Frontiers in neuroscience 2013;7:85
6. Jiao H, Arner P, Hoffstedt J, Brodin D, Dubern B, Czernichow S, van't Hooft F, Axelsson T, Pedersen O, Hansen T, Sorensen TI, Hebebrand J, Kere J, Dahlman-Wright K, Hamsten A, Clement K, Dahlman I: Genome wide association study identifies KCNMA1 contributing to human obesity. BMC medical genomics 2011;4:51
7. Hu H, He ML, Tao R, Sun HY, Hu R, Zang WJ, Yuan BX, Lau CP, Tse HF, Li GR: Characterization of ion channels in human preadipocytes. Journal of cellular physiology 2009;218:427-435
8. Zhang XH, Zhang YY, Sun HY, Jin MW, Li GR: Functional ion channels and cell proliferation in 3T3-L1 preadipocytes. Journal of cellular physiology 2012;227:1972-1979
9. Dopico AM, Bukiya AN: Lipid regulation of BK channel function. Frontiers in physiology 2014;5:312
10. Martin P, Moncada M, Enrique N, Asuaje A, Valdez Capuccino JM, Gonzalez C, Milesi V: Arachidonic acid activation of BKCa (Slo1) channels associated to the beta1-subunit in human vascular smooth muscle cells. Pflugers Archiv : European journal of physiology 2014;466:1779-1792
11. Hoshi T, Tian Y, Xu R, Heinemann SH, Hou S: Mechanism of the modulation of BK potassium channel complexes with different auxiliary subunit compositions by the omega-3 fatty acid DHA. Proceedings of the National Academy of Sciences of the United States of America 2013;110:4822-4827
12. Lynch FM, Withers SB, Yao Z, Werner ME, Edwards G, Weston AH, Heagerty AM: Perivascular adipose tissue-derived adiponectin activates BK(Ca) channels to induce anticontractile responses. American journal of physiology Heart and circulatory physiology 2013;304:H786-795
13. Climent B, Simonsen U, Rivera L: Effects of obesity on vascular potassium channels. Current vascular pharmacology 2014;12:438-452
14. Brunton PJ, Sausbier M, Wietzorrek G, Sausbier U, Knaus HG, Russell JA, Ruth P, Shipston MJ: Hypothalamic-pituitary-adrenal axis hyporesponsiveness to restraint stress in mice deficient for large-conductance calcium- and voltage-activated potassium (BK) channels. Endocrinology 2007;148:5496-5506
15. Dufer M, Neye Y, Horth K, Krippeit-Drews P, Hennige A, Widmer H, McClafferty H, Shipston MJ, Haring HU, Ruth P, Drews G: BK channels affect glucose homeostasis and cell viability of murine pancreatic beta cells. Diabetologia 2011;54:423-432
16. Peters A, Schweiger U, Fruhwald-Schultes B, Born J, Fehm HL: The neuroendocrine control of glucose allocation. Experimental and clinical endocrinology & diabetes : official journal, German Society of Endocrinology [and] German Diabetes Association 2002;110:199-211
17. Shanley LJ, O'Malley D, Irving AJ, Ashford ML, Harvey J: Leptin inhibits epileptiform-like activity in rat hippocampal neurones via PI 3-kinase-driven activation of BK channels. The Journal of physiology 2002;545:933-944

18. Gavello D, Vandael D, Gosso S, Carbone E, Carabelli V: Dual action of leptin on rest-firing and stimulated catecholamine release via phosphoinositide 3-kinase-driven BK channel up-regulation in mouse chromaffin cells. The Journal of physiology 2015;593:4835-4853
19. Schneeberger M, Gomis R, Claret M: Hypothalamic and brainstem neuronal circuits controlling homeostatic energy balance. The Journal of endocrinology 2014;220:T25-46
20. Sausbier U, Sausbier M, Sailer CA, Arntz C, Knaus HG, Neuhuber W, Ruth P: Ca2+ -activated K+ channels of the BK-type in the mouse brain. Histochemistry and cell biology 2006;125:725-741
21. Chang CP, Dworetzky SI, Wang J, Goldstein ME: Differential expression of the alpha and beta subunits of the large-conductance calcium-activated potassium channel: implication for channel diversity. Brain research Molecular brain research 1997;45:33-40
22. Sausbier M, Arntz C, Bucurenciu I, Zhao H, Zhou XB, Sausbier U, Feil S, Kamm S, Essin K, Sailer CA, Abdullah U, Krippeit-Drews P, Feil R, Hofmann F, Knaus HG, Kenyon C, Shipston MJ, Storm JF, Neuhuber W, Korth M, Schubert R, Gollasch M, Ruth P: Elevated blood pressure linked to primary hyperaldosteronism and impaired vasodilation in BK channel-deficient mice. Circulation 2005;112:60-68
23. Sassmann A, Offermanns S, Wettschureck N: Tamoxifen-inducible Cre-mediated recombination in adipocytes. Genesis 2010;48:618-625
24. Muzumdar MD, Tasic B, Miyamichi K, Li L, Luo L: A global double-fluorescent Cre reporter mouse. Genesis 2007;45:593-605
25. Lukowski R, Rybalkin SD, Loga F, Leiss V, Beavo JA, Hofmann F: Cardiac hypertrophy is not amplified by deletion of cGMP-dependent protein kinase I in cardiomyocytes. Proceedings of the National Academy of Sciences of the United States of America 2010;107:5646-5651
26. Jennissen K, Haas B, Mitschke MM, Siegel F, Pfeifer A: Analysis of cGMP signaling in adipocytes. Methods Mol Biol 2013;1020:175-192
27. Leiss V, Illison J, Domes K, Hofmann F, Lukowski R: Expression of cGMP-dependent protein kinase type I in mature white adipocytes. Biochemical and biophysical research communications 2014;452:151-156
28. Leiss V, Friebe A, Welling A, Hofmann F, Lukowski R: Cyclic GMP kinase I modulates glucagon release from pancreatic alpha-cells. Diabetes 2011;60:148-156
29. Sausbier M, Hu H, Arntz C, Feil S, Kamm S, Adelsberger H, Sausbier U, Sailer CA, Feil R, Hofmann F, Korth M, Shipston MJ, Knaus HG, Wolfer DP, Pedroarena CM, Storm JF, Ruth P: Cerebellar ataxia and Purkinje cell dysfunction caused by Ca2+-activated K+ channel deficiency. Proceedings of the National Academy of Sciences of the United States of America 2004;101:9474-9478
30. Soltysinska E, Bentzen BH, Barthmes M, Hattel H, Thrush AB, Harper ME, Qvortrup K, Larsen FJ, Schiffer TA, Losa-Reyna J, Straubinger J, Kniess A, Thomsen MB, Bruggemann A, Fenske S, Biel M, Ruth P, Wahl-Schott C, Boushel RC, Olesen SP, Lukowski R: KCNMA1 encoded cardiac BK channels afford protection against ischemia-reperfusion injury. PloS one 2014;9:e103402
31. Perry CA, Pravetoni M, Teske JA, Aguado C, Erickson DJ, Medrano JF, Lujan R, Kotz CM, Wickman K: Predisposition to late-onset obesity in GIRK4 knockout mice. Proceedings of the National Academy of Sciences of the United States of America 2008;105:8148-8153
32. Park YB, Choi YJ, Park SY, Kim JY, Kim SH, Song DK, Won KC, Kim YW: ATP-Sensitive Potassium Channel-Deficient Mice Show Hyperphagia but Are Resistant to Obesity. Diabetes & metabolism journal 2011;35:219-225
33. Plum L, Ma X, Hampel B, Balthasar N, Coppari R, Munzberg H, Shanabrough M, Burdakov D, Rother E, Janoschek R, Alber J, Belgardt BF, Koch L, Seibler J, Schwenk F, Fekete C, Suzuki A, Mak TW, Krone W, Horvath TL, Ashcroft FM, Bruning JC: Enhanced

PIP3 signaling in POMC neurons causes KATP channel activation and leads to diet-sensitive obesity. The Journal of clinical investigation 2006;116:1886-1901
34. Yang MJ, Wang F, Wang JH, Wu WN, Hu ZL, Cheng J, Yu DF, Long LH, Fu H, Xie N, Chen JG: PI3K integrates the effects of insulin and leptin on large-conductance Ca2+-activated K+ channels in neuropeptide Y neurons of the hypothalamic arcuate nucleus. American journal of physiology Endocrinology and metabolism 2010;298:E193-201
35. Tucker K, Overton JM, Fadool DA: Kv1.3 gene-targeted deletion alters longevity and reduces adiposity by increasing locomotion and metabolism in melanocortin-4 receptor-null mice. Int J Obes (Lond) 2008;32:1222-1232
36. Xu J, Koni PA, Wang P, Li G, Kaczmarek L, Wu Y, Li Y, Flavell RA, Desir GV: The voltage-gated potassium channel Kv1.3 regulates energy homeostasis and body weight. Human molecular genetics 2003;12:551-559
37. Kalra SP, Dube MG, Pu S, Xu B, Horvath TL, Kalra PS: Interacting appetite-regulating pathways in the hypothalamic regulation of body weight. Endocrine reviews 1999;20:68-100
38. Upadhyay SK, Eckel-Mahan KL, Mirbolooki MR, Tjong I, Griffey SM, Schmunk G, Koehne A, Halbout B, Iadonato S, Pedersen B, Borrelli E, Wang PH, Mukherjee J, Sassone-Corsi P, Chandy KG: Selective Kv1.3 channel blocker as therapeutic for obesity and insulin resistance. Proceedings of the National Academy of Sciences of the United States of America 2013;110:E2239-2248
39. Rutkowski JM, Stern JH, Scherer PE: The cell biology of fat expansion. The Journal of cell biology 2015;208:501-512
40. Sopasakis VR, Sandqvist M, Gustafson B, Hammarstedt A, Schmelz M, Yang X, Jansson PA, Smith U: High local concentrations and effects on differentiation implicate interleukin-6 as a paracrine regulator. Obesity research 2004;12:454-460
41. Eder K, Baffy N, Falus A, Fulop AK: The major inflammatory mediator interleukin-6 and obesity. Inflammation research : official journal of the European Histamine Research Society [et al] 2009;58:727-736
42. Harkins JM, Moustaid-Moussa N, Chung YJ, Penner KM, Pestka JJ, North CM, Claycombe KJ: Expression of interleukin-6 is greater in preadipocytes than in adipocytes of 3T3-L1 cells and C57BL/6J and ob/ob mice. The Journal of nutrition 2004;134:2673-2677
43. Bartelt A, Heeren J: Adipose tissue browning and metabolic health. Nature reviews Endocrinology 2014;10:24-36
44. Pfeifer A, Hoffmann LS: Brown, beige, and white: the new color code of fat and its pharmacological implications. Annual review of pharmacology and toxicology 2015;55:207-227
45. Neal JW, Clipstone NA: Calcineurin mediates the calcium-dependent inhibition of adipocyte differentiation in 3T3-L1 cells. The Journal of biological chemistry 2002;277:49776-49781
46. Hu R, He ML, Hu H, Yuan BX, Zang WJ, Lau CP, Tse HF, Li GR: Characterization of calcium signaling pathways in human preadipocytes. Journal of cellular physiology 2009;220:765-770
47. Shi H, Halvorsen YD, Ellis PN, Wilkison WO, Zemel MB: Role of intracellular calcium in human adipocyte differentiation. Physiological genomics 2000;3:75-82
48. Oguri A, Tanaka T, Iida H, Meguro K, Takano H, Oonuma H, Nishimura S, Morita T, Yamasoba T, Nagai R, Nakajima T: Involvement of CaV3.1 T-type calcium channels in cell proliferation in mouse preadipocytes. American journal of physiology Cell physiology 2010;298:C1414-1423
49. Jensen B, Farach-Carson MC, Kenaley E, Akanbi KA: High extracellular calcium attenuates adipogenesis in 3T3-L1 preadipocytes. Experimental cell research 2004;301:280-292

50. Sun W, Uchida K, Suzuki Y, Zhou Y, Kim M, Takayama Y, Takahashi N, Goto T, Wakabayashi S, Kawada T, Iwata Y, Tominaga M: Lack of TRPV2 impairs thermogenesis in mouse brown adipose tissue. EMBO reports 2016;17:383-399
51. Ma S, Yu H, Zhao Z, Luo Z, Chen J, Ni Y, Jin R, Ma L, Wang P, Zhu Z, Li L, Zhong J, Liu D, Nilius B: Activation of the cold-sensing TRPM8 channel triggers UCP1-dependent thermogenesis and prevents obesity. Journal of molecular cell biology 2012;4:88-96
52. Zhang LL, Yan Liu D, Ma LQ, Luo ZD, Cao TB, Zhong J, Yan ZC, Wang LJ, Zhao ZG, Zhu SJ, Schrader M, Thilo F, Zhu ZM, Tepel M: Activation of transient receptor potential vanilloid type-1 channel prevents adipogenesis and obesity. Circulation research 2007;100:1063-1070
53. Worrall DS, Olefsky JM: The effects of intracellular calcium depletion on insulin signaling in 3T3-L1 adipocytes. Mol Endocrinol 2002;16:378-389
54. Yang H, Cui J: BK Channels. In *Handbook of Ion Channels* Zheng J, Trudeau MC, Eds., CRC Press, 2015, p. 227-240
55. Ye L, Kleiner S, Wu J, Sah R, Gupta RK, Banks AS, Cohen P, Khandekar MJ, Bostrom P, Mepani RJ, Laznik D, Kamenecka TM, Song X, Liedtke W, Mootha VK, Puigserver P, Griffin PR, Clapham DE, Spiegelman BM: TRPV4 is a regulator of adipose oxidative metabolism, inflammation, and energy homeostasis. Cell 2012;151:96-110
56. Earley S, Heppner TJ, Nelson MT, Brayden JE: TRPV4 forms a novel Ca2+ signaling complex with ryanodine receptors and BKCa channels. Circulation research 2005;97:1270-1279
57. Fernandez-Fernandez JM, Andrade YN, Arniges M, Fernandes J, Plata C, Rubio-Moscardo F, Vazquez E, Valverde MA: Functional coupling of TRPV4 cationic channel and large conductance, calcium-dependent potassium channel in human bronchial epithelial cell lines. Pflugers Archiv : European journal of physiology 2008;457:149-159
58. Che H, Yue J, Tse HF, Li GR: Functional TRPV and TRPM channels in human preadipocytes. Pflugers Archiv : European journal of physiology 2014;466:947-959
59. Zhou XB, Arntz C, Kamm S, Motejlek K, Sausbier U, Wang GX, Ruth P, Korth M: A molecular switch for specific stimulation of the BKCa channel by cGMP and cAMP kinase. The Journal of biological chemistry 2001;276:43239-43245
60. Zhou XB, Wulfsen I, Utku E, Sausbier U, Sausbier M, Wieland T, Ruth P, Korth M: Dual role of protein kinase C on BK channel regulation. Proceedings of the National Academy of Sciences of the United States of America 2010;107:8005-8010
61. Carmen GY, Victor SM: Signalling mechanisms regulating lipolysis. Cellular signalling 2006;18:401-408

**Figure Legends**

***Figure 1:*** **Global lack of BK channels protects from overwhelming body weight (BW) gain and excessive fat accumulation.**

**(A)** Body weight (BW) increase of $BK^{+/+}$ (blue) and $BK^{L1/L1}$ (red) mice that received a control diet (CD) (n=12-14 mice per time-point; open data points) or 45% high-fat diet (HFD) (n=23-25 mice per time-point, filled data points) for 18 weeks. **(B)** Body-composition of $BK^{+/+}$ and $BK^{L1/L1}$ mice after 18 weeks of dietary feeding was analyzed using the Soxhlet extraction method (n=4-7 mice per genotype). Representative images of **(C)** $BK^{+/+}$ and $BK^{L1/L1}$ mice after 18 weeks of CD- or HFD dietary feeding. **(D)** Fat mass of different white (WAT) and brown (BAT) adipose tissue depots of $BK^{+/+}$ and $BK^{L1/L1}$ mice fed either a CD (n=6-9 mice per fat depot) or HFD (n=9-16 mice per fat depot). Fat masses were normalized to tibia length (Suppl. Fig. 1F) to overcome growth differences between $BK^{+/+}$ and $BK^{L1/L1}$ mice that are not related to gain of body adiposity. Relative mRNA-expression of the BK-channel alpha subunit in **(E)** epididymal WAT (eWAT) and **(F)** subcutaneous inguinal WAT (iWAT) of 10 week old $BK^{+/+}$ and $BK^{L1/L1}$ mice. Glyceraldehyde-3-phosphate dehydrogenase mRNA levels were used as a reference to normalize the data, which are presented as means ± SEM. Statistical difference between the two genotypes is indicated by * P<0.05, ** P<0.01. Representative cryo-sections of **(G)** eWAT and **(H)** iWAT stained for the BK alpha-subunit (upper panels) using a specific BK channel antibody. As negative control frozen tissue sections without the primary BK antibody were processed (lower panels). (G, H) Scale bars represent 200 µm.

Data were analyzed using the 2-way ANOVA test (A) or Student‘s t-test (B, D-F) and are presented as means ± SEM. Statistical difference between the two genotypes is indicated by * P<0.05, ** P<0.01, *** P<0.001. *Abbreviations used:* Epididymal WAT (eWAT); interscapular WAT (intWAT); interscapular BAT (intBAT); mesenteric WAT (mesWAT); subcutaneous inguinal WAT (iWAT).

***Figure 2:*** **Accelerated growth of BK-negative epididymal WAT (eWAT)-derived pre-adipocytes.**

Representative Oil-red-O (ORO) staining of eWAT-derived pre-adipocytes in **(A)** high magnification and **(B)** as overviews screen after 14 days of adipogenic differentiation revealing higher numbers of mature adipocytes in $BK^{L1/L1}$ in comparison to $BK^{+/+}$ cells. **(C)** The increased adipogenic potential in $BK^{L1/L1}$ (red) was confirmed by analyzing ORO-incorporation quantitatively at 518 nm (n=3 independent *in vitro* assays per genotype). **(D, E)**

Representative ORO staining of inguinal WAT (iWAT)-derived pre-adipocytes after 14 days of adipogenic differentiation. Scale bars (A, D) represent 100 µm. **(E, F)** Based on the ORO-incorporation assay maturation of iWAT-derived $BK^{+/+}$ and $BK^{L1/L1}$ pre-adipocytes was not different between the genotypes (n=7-8 independent *in vitro* assays per genotype). **(G)** Representative growth of eWAT-derived pre-adipocytes examined in real-time using an impedance-based setup. Lack of BK channels (red) in eWAT-derived pre-adipocytes resulted in accelerated growth properties at different cell concentrations tested as compared to wild-type cells (blue). **(H)** A pharmacological approach to block the BK channel using 1 µM paxilline confirmed the BK-dependent growth capacity of eWAT-derived pre-adipocytes. **(I)** Up-regulation of GLUT4 and BK channel mRNA and **(J)** protein levels following differentiation of eWAT murine pre-adipocytes (pre-adipo) to adipocytes (adipo) (n=3 independent experiments per group). **(K)** Pre-adipocyte cells display a small paxilline-sensitive (1 µM) outward whole-cell BK potassium current determined under physiological potassium gradients (n=8 cells) that was significantly increased upon adipogenic differentiation for 14 days (n=12 cells).

***Figure 3:*** **Spatiotemporal ablation of fat cell BK channels using the *adipoqCreERT2*$^{tg/+}$ recombination system.**

Recombination efficiency was determined by a change from red (Cy3-channel) to green (FITC-channel) fluorescence using the *ROSA26-Tomato*$^{tom/+}$ (tom/+) Cre-reporter mouse line. **(A)** Analysis of eWAT and **(B)** subcutaneous iWAT derived from double-transgenic *adipoqCreER*$^{tg/+}$*; ROSA26-Tomato*$^{tom/+}$ (tg/+; tom/+) mice with or without tamoxifen (TAM) injections in comparison to wildtype age-matched littermate male control mice (+/+; +/+). **(C)** Genomic PCR-analysis of the *adipoqCreERT2*$^{tg/+}$-mediated recombination of the pre-mutant BK gene locus in different tissues. PCR products amplified from the loxP-flanked (L2 allele with two loxP sites; two black triangles flanking a closed box), wild type (+ allele; closed black box), and knock-out (L1 allele with one loxP site; one black triangle) alleles of representative *adipoqCreERT2*$^{tg/+}$; $BK^{+/L2}$ (*adipoqBK*$^{+/L2}$) animals. Conversion of the loxP-flanked L2 allele to the L1 allele was only observed in fat cell depots after injecting tamoxifen (+), whereas with saline (-) treatment we did not find evidence for unspecific Cre activity. Recombination was analyzed 14 days after the beginning of tamoxifen or saline injections in 10 weeks old mice. The size of the PCR amplicons were 577 bp, 466 bp and 132 bp for the floxed, WT and knockout allele, respectively. *Abbreviations used:* Pancreas (P); liver (L); hypothalamus (H); bulb (B); cerebellum (C); rest of brain (Br); heart (He); skeletal muscle

(S); duodenum (D); epididymal white adipose tissue (eWAT); subcutaneous inguinal white adipose tissue (iWAT) and brown adipose tissue (BAT); marker (M). **(D)** Quantitative mRNA analysis of the BK mRNA in eWAT and iWAT of TAM-injected *adipoqCreER*$^{tg/+}$; *BK*$^{+/L2}$ control mice (n= 5 for eWAT and iWAT) and age and littermatched *adipoqCreER*$^{tg/+}$; *BK*$^{L1/L2}$ tissue-specific mutants n= 7 for eWAT and n=4 iWAT). Analysis of the frequency and distribution of the adiponectin-CreERT2-mediated recombination after TAM injections in **(E)** eWAT and **(F)** iWAT of *adipoqCreER*$^{tg/+}$; *BK*$^{+/L2}$ (*adipoqBK*$^{+/L2}$) and *adipoqCreER*$^{tg/+}$; *BK*$^{L1/L2}$ (*adipoqBK*$^{L1/L2}$) mice using a specific BK channel antibody (+anti-BK; upper panels). A parallel analysis of serial eWAT and iWAT sections from both genotypes was performed to establish the background fluorescence in the absence of BK-specific antibodies (-anti-BK; lower panels). Scale bars represent 50 μm.

***Figure 4:*** **Reduced BW gain in *adipoqBK*$^{L1/L2}$ mice receiving a 60% HFD feeding.**
**(A)** Control diet (CD) feeding protocol. Male *adipoqCreER*$^{tg/+}$; *BK*$^{L1/L2}$ (*adipoqBK*$^{L1/L2}$) and *adipoqCreER*$^{tg/+}$; *BK*$^{+/L2}$ (*adipoqBK*$^{+/L2}$) were injected prior to the dietary feeding with tamoxifen (TAM) for 5 consecutive days at an age of 8 weeks, which induced a specific and efficient ablation of the BK channel in various adipose tissues (see also Fig. 3). Upon 2 weeks of adaption to the CD, CD diet feeding was continued or **(B)** mice revived a HFD for 18 weeks (prevention study). In an alternative approach additional groups of *adipoqBK*$^{L1/L2}$ and *adipoqBK*$^{+/L2}$ mice were subjected to the same feeding protocol, but tamoxifen was injected at an age of 19 weeks ($TAM_{19}$) when over-weight has already been established. Food intake of *adipoqBK*$^{L1/L2}$ (red) and *adipoqBK*$^{+/L2}$ (blue) mice were analyzed, using modified metabolic cages as described in the methods section either **(C)** at the beginning (n=4-6 mice per genotype) or **(D)** at the end of the respective dietary feeding (n=3-5 mice per genotype). BW development under **(E)** CD feeding (n=12-20 per genotype/time-point) and **(F)** HFD feeding (n=24-29 mice per genotype/time-point). Difference (ΔBW) between the initial BW (at week 10) and the BW at week 30 in *adipoqBK*$^{L1/L2}$ (red) and *adipoqBK*$^{+/L2}$ (blue) mice under **(G)** CD and **(H)** HFD feeding conditions (n=12-15 per genotype for CD, n=24-26 per genotype for HFD). **(I)** Tamoxifen was injected for 5 consecutive days at an age of 19 week when a HFD-induced BW gain in *adipoqBK*$^{L1/L2}$ (red) and *adipoqBK*$^{+/L2}$ (blue) mice was already established to test the therapeutic potential of WAT BK inactivation (n=17-22 mice per genotype/time-point). The final BW between the two genotypes was significantly different (* $P<0.05$).

***Figure 5:*** **Reduced fat accumulation and smaller fat depots in *adipoqBK$^{L1/L2}$* mice fed a 60% high-fat diet (HFD).**

Mass of different white (WAT) and brown (BAT) adipose tissue depots of male *adipoqBK$^{L1/L2}$* (red) and *adipoqBK$^{+/L2}$* (blue) mice examined after 18 weeks of **(A)** control diet (CD) or **(B)** HFD feeding (n=12-15 per genotype for CD, n=24-26 per genotype for HFD). Body-composition of *adipoqBK$^{+/L2}$* and *adipoqBK$^{L1/L2}$* at an age of 30 weeks **(C)** after CD and **(D)** after HFD feeding. Total body fat was extracted using the soxhlet extraction method (n=3 per genotype for CD, n=4-7 per genotype for HFD). **(E-G)** Representative pictures of *adipoqBK$^{+/L2}$* and *adipoqBK$^{L1/L2}$* mice and selected fat depots after 18 weeks on CD. **(E)** View from back, **(F)** front view with opened abdominal cavity and **(G)** magnification of BAT, eWAT and iWAT. All data were analyzed using the Student‘s t-test and are presented as means ± SEM (* P<0.05). **(E-G)** Scale bars represent 2 cm. *Abbreviations used:* Epididymal WAT (eWAT), interscapular WAT (intWAT), interscapular BAT (intBAT), total interscapular adipose tissue (intAT), mesenteric WAT (mesWAT), subcutaneous inguinal WAT (iWAT) and total investigated adipose depots (total).

***Figure 6:*** **Fat cell hyperplasia and improved glucose handling in *adipoqBK$^{L1/L2}$* mice.**

**(A)** Average cell size of inguinal WAT (iWAT) of male *adipoqBK$^{+/L2}$* and *adipoqBK$^{L1/L2}$* mice after 18 weeks of HFD was examined in serial cryo-sections by measuring the circumference of cells in central and peripheral regions of the respective depots. **(B)** Classification of average cell sizes (as an indicator of adipose cell number) in *adipoqBK$^{+/L2}$* and *adipoqBK$^{L1/L2}$* iWAT, prior diet (PD) and after 18 weeks of control diet (CD) or 60% high-fat diet (HFD) feeding. **(C)** Representative cryo-sections of iWAT derived from *adipoqBK$^{+/L2}$* (blue) and *adipoqBK$^{L1/L2}$* (red) PD or after either 18 weeks of CD or HFD. Scale bars represent 100 µm**.** Relative **(D)** mRNA-expression and **(E)** serum levels of interleukin-6 (IL-6) a marker for adipose tissue inflammation and serum levels of **(F)** adiponectin and **(G)** leptin determined after 18 weeks of CD (open bars) and/or HFD (closed bars) feeding in *adipoqBK$^{+/L2}$* (blue) and *adipoqBK$^{L1/L2}$* (red) mice. Blood-glucose (BG) levels were monitored before as well as 15, 30, 60 and 120 minutes after i.p. injection of 2 g/kg glucose **(H)** after 18 weeks of HFD-feeding and **(I)** prior the respective diet. **(J)** Plasma insulin levels at baseline (0 min) and during the intraperitoneal glucose-tolerance-test (15 to 120 min post injection) in *adipoqBK$^{L2/+}$* (blue, n=6) and *adipoqBK$^{L1/L2}$* (red, n=8) mice after 18 weeks of HFD-feeding. All data (A, D-J) were examined using the Student‘s t-test and are presented as means ± SEM (* P<0.05, ** P<0.01).

***Figure 7:*** **Increased UCP1 levels and body temperature in HFD-fed *adipoqBK$^{L1/L2}$* mice**

(**A**) UCP1 expression analysis (brown staining in left panels) in frozen tissue sections derived from HFD-fed *adipoqBK$^{+/L2}$* and *adipoqBK$^{L1/L2}$* iWAT. As negative control sections derived from the same fat pads were processed in the absence of the primary UCP1 antibody (right panels). (**B**) Representative UCP1immunoblot of iWAT protein lysates derived from HFD-fed *adipoqBK$^{+/L2}$* and *adipoqBK$^{L1/L2}$* mice. Equal loading of the gel was verified by co-detection of glyceraldehyde-3-phosphate dehydrogenase (GAPDH). (**C**) Quantification of the immunoblot data shown in (B). UCP1 protein levels were normalized to the expression of GAPDH in *adipoqBK$^{+/L2}$* (closed blue bars; n=3) and *adipoqBK$^{L1/L2}$* (closed red bars; n=4) iWAT samples. (**D**) Telemetric sensors were used to measure the body core temperature of a subset of *adipoqBK$^{+/L2}$* and *adipoqBK$^{L1/L2}$* mice that received the HFD-feeding. All data (C, D) were assessed using the Student‘s *t*-test and are presented as means ± SEM. * $P<0.05$, ** $P<0.01$.

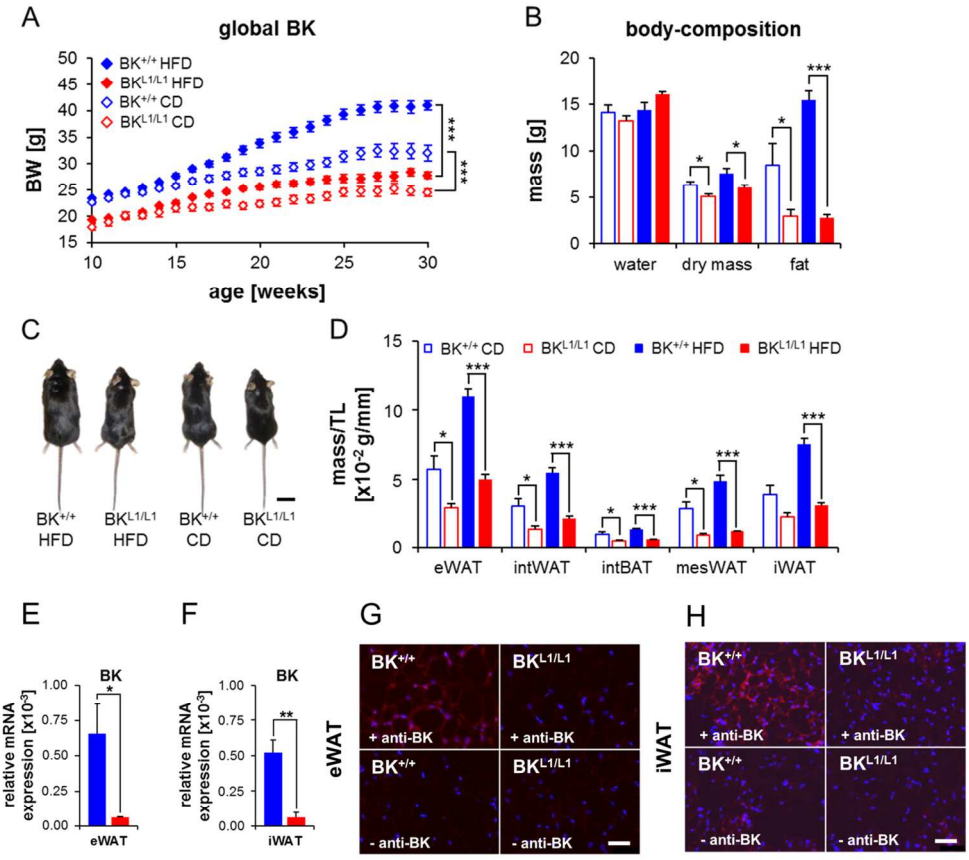


Figure 1
Figure 1
132x123mm (300 x 300 DPI)

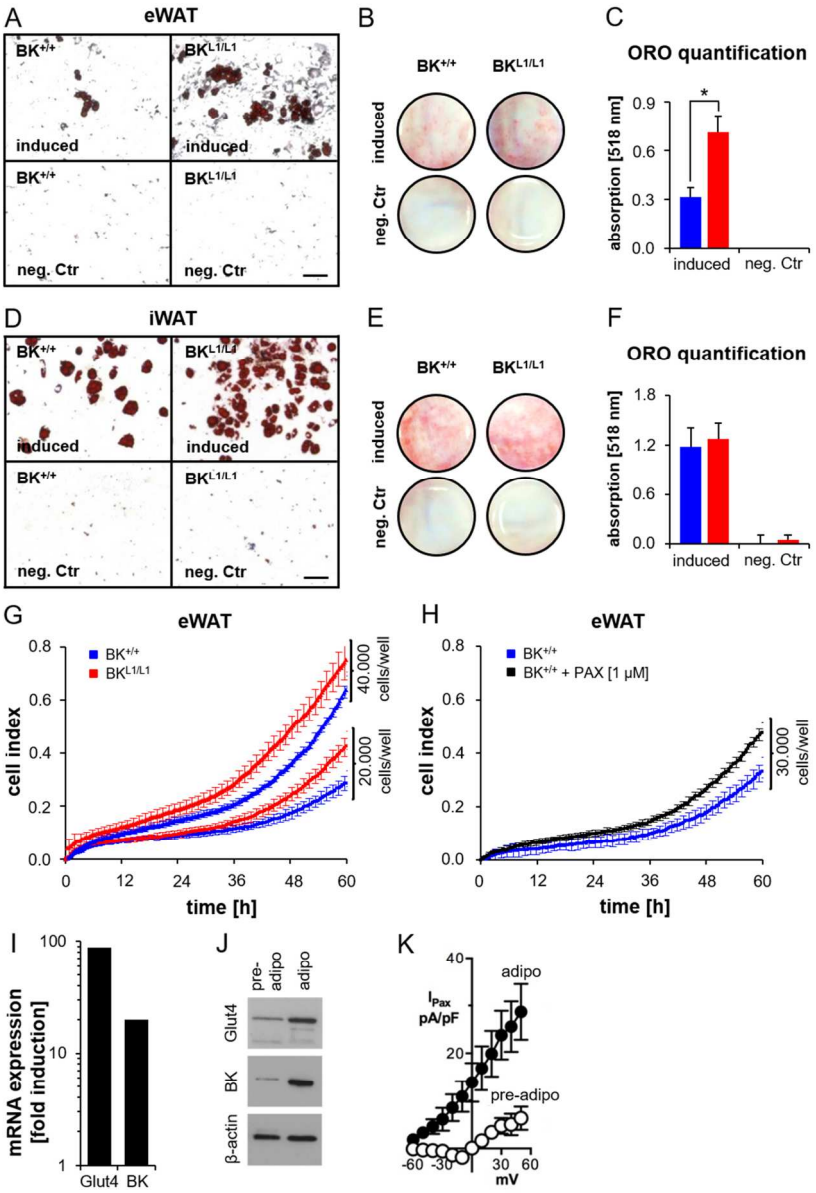


Figure 2
Figure 2
184x257mm (300 x 300 DPI)

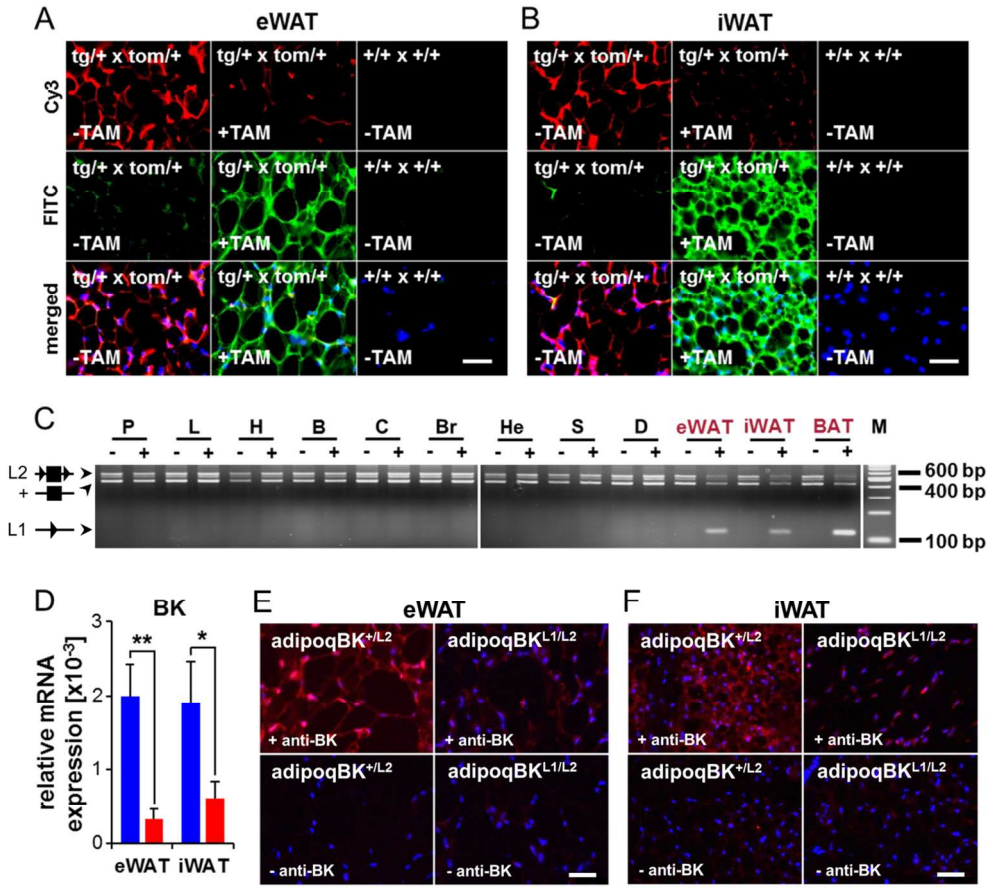


Figure 3
Figure 3
121x111mm (300 x 300 DPI)

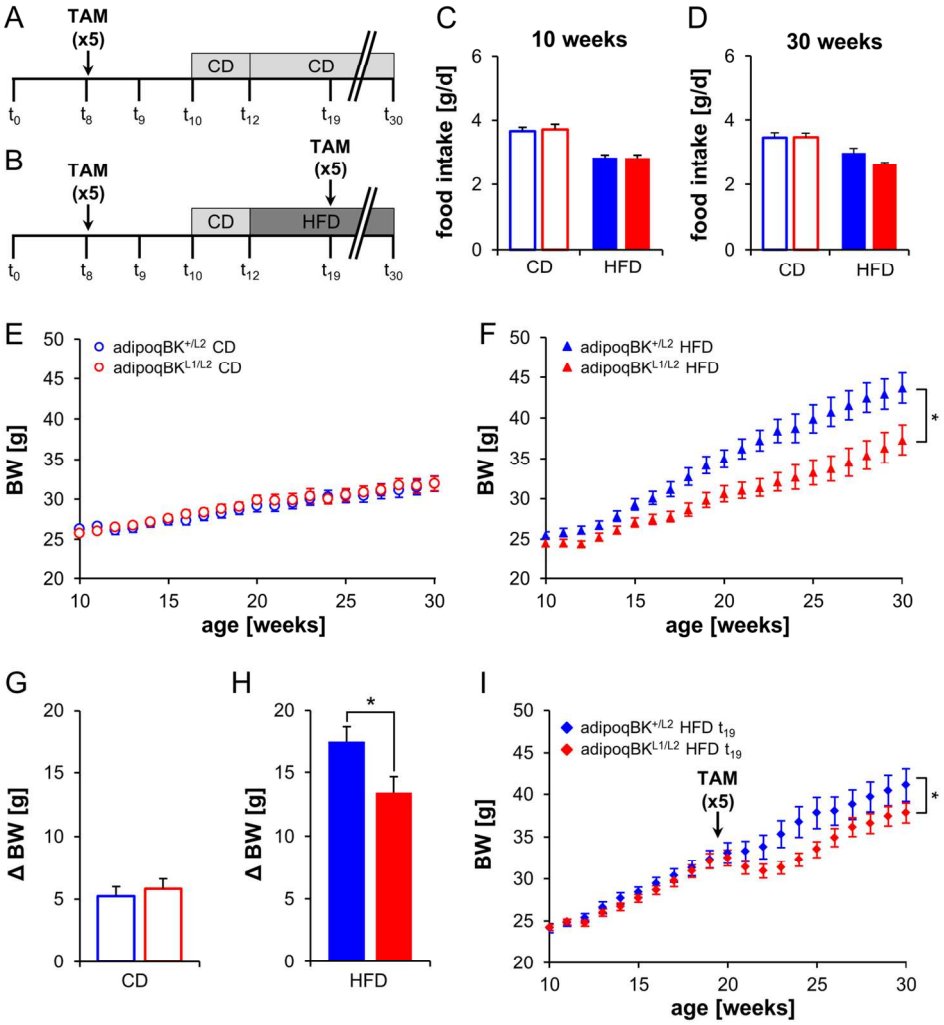


Figure 4
Figure 4
156x170mm (300 x 300 DPI)

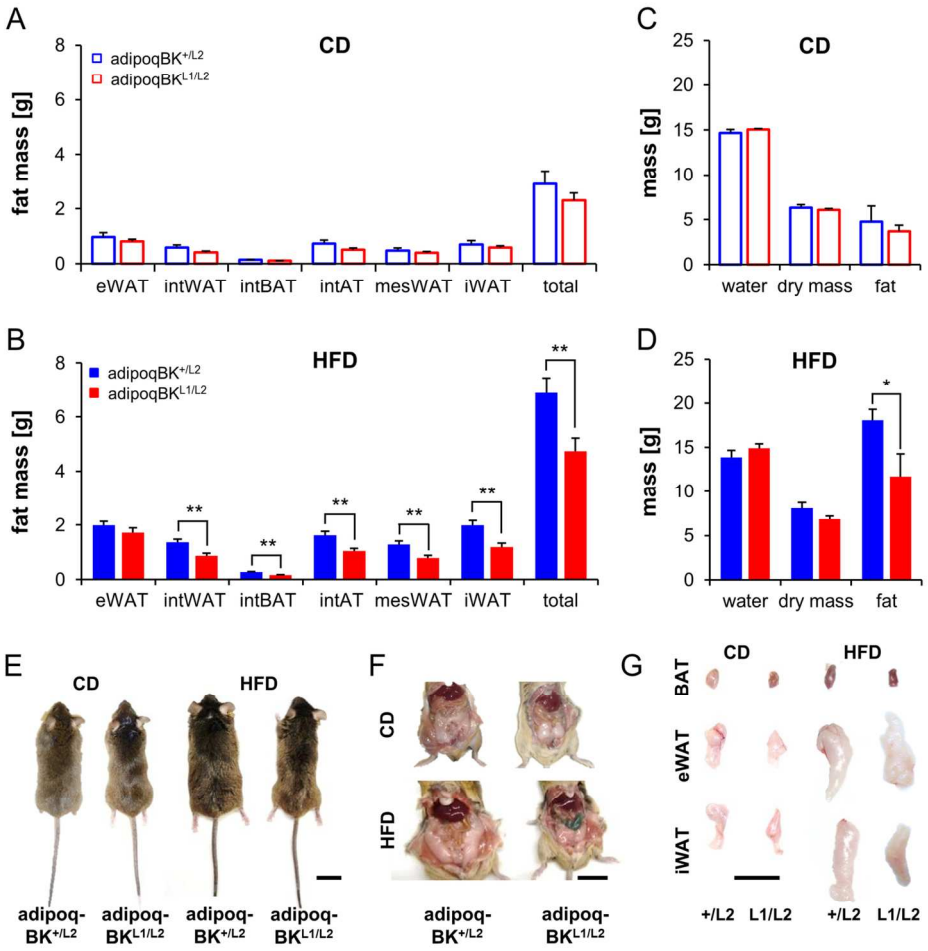


Figure 5
Figure 5
147x151mm (300 x 300 DPI)

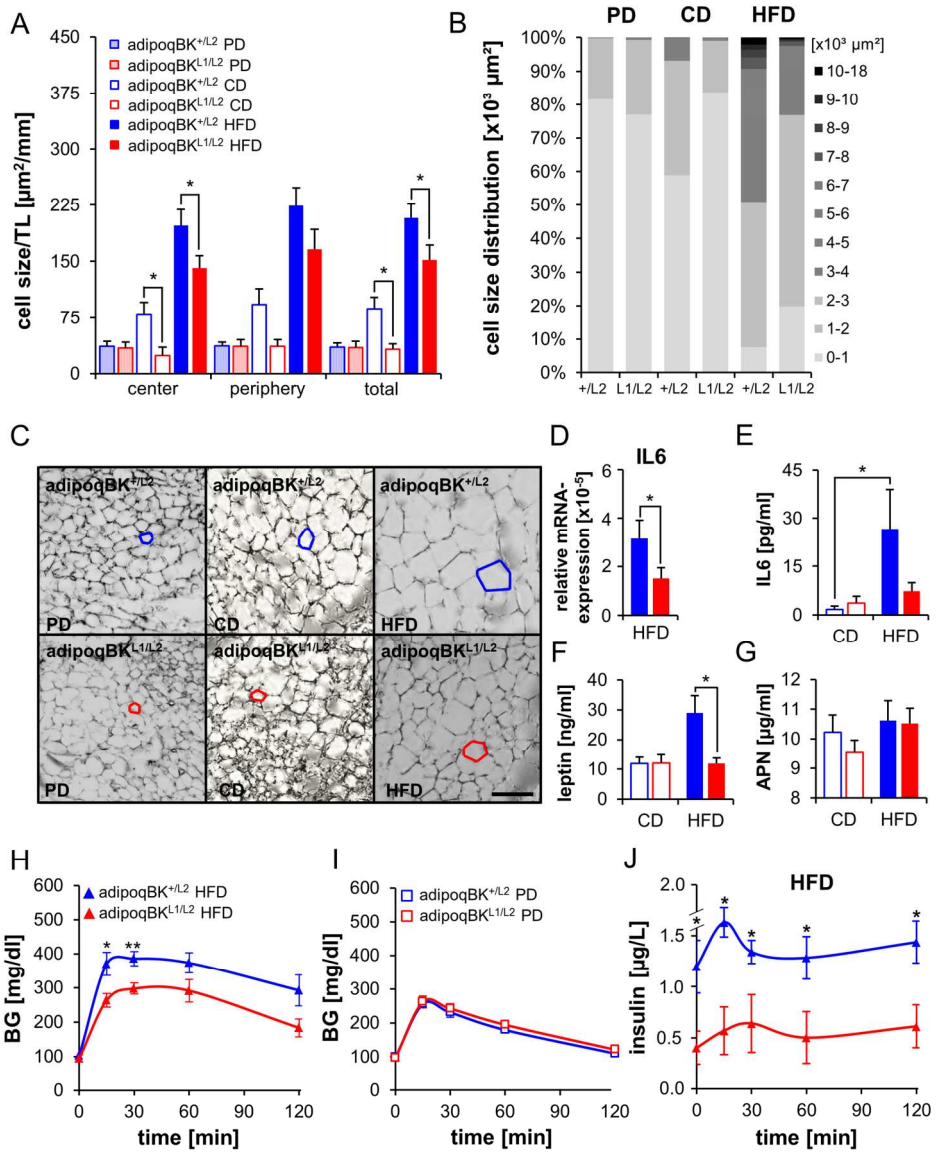


Figure 6
Figure 6
176x218mm (300 x 300 DPI)

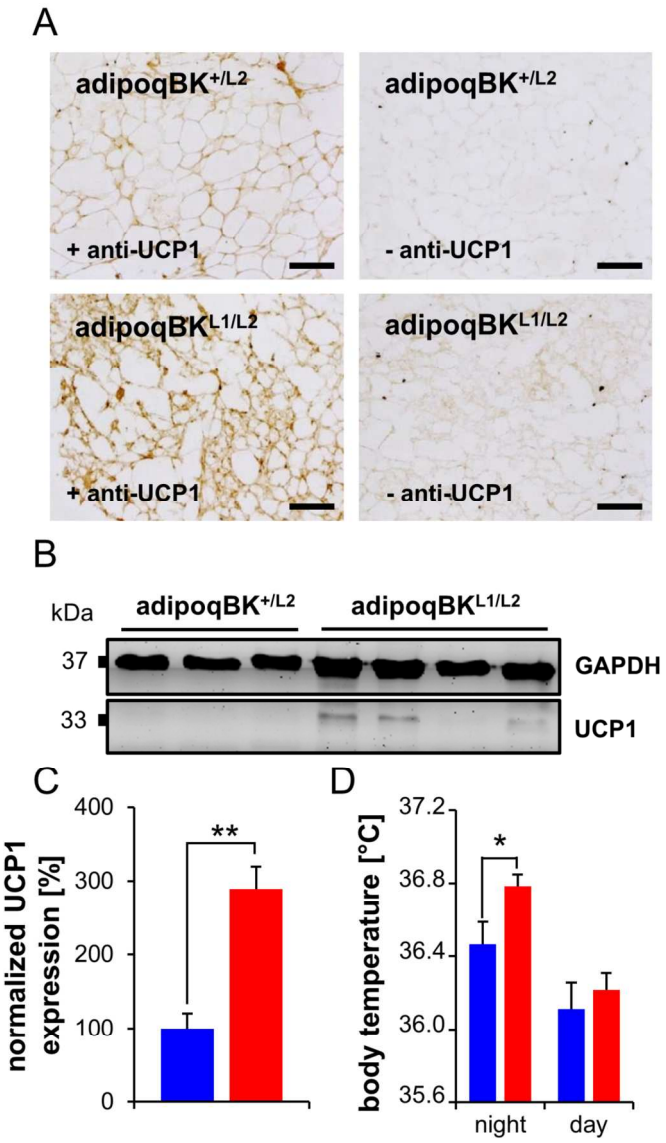


Figure 7
Figure 7
133x217mm (300 x 300 DPI)

# Obesogenic and diabetogenic effects of high-calorie nutrition require adipocyte BK channels

Julia Illison[1], Lijun Tian[2], Heather McClafferty[2], Martin Werno[3], Luke H. Chamberlain[3], Veronika Leiss[4], Antonia Sassmann[5], Stefan Offermanns[5], Peter Ruth[1], Michael J. Shipston[2], Robert Lukowski[1, §]

[1]Pharmakologie, Toxikologie und Klinische Pharmazie, Institut für Pharmazie, Tübingen, Germany
[2]Centre for Integrative Physiology, College of Medicine and Veterinary Medicine, University of Edinburgh, Edinburgh, UK
[3]Strathclyde Institute of Pharmacy and Biomedical Sciences, Strathclyde University, Glasgow, UK
[4]Department of Pharmacology and Experimental Therapy, Institute of Experimental and Clinical Pharmacology and Toxicology, University Hospital Tuebingen, Tuebingen, Germany
[5]Department of Pharmacology, Max-Planck-Institute for Heart and Lung Research, Bad Nauheim, Germany

[§]**Corresponding author:** Robert Lukowski, Department of Pharmacology, Toxicology and Clinical Pharmacy, Institute of Pharmacy, University of Tübingen, Tel. +49 7071 29 74550, Fax +49 7071 29 2476, E-mail: robert.lukowski@uni-tuebingen.de

**Running Title:** Adipocyte BK protects from overwhelming BW gain

**Supplemental information:** Supplemental Figure Legends (1-4)

**Suppl. Figure Legends**

***Suppl. Fig. 1:*** Change in **(A)** absolute and **(B)** percental body weight (BW) of global BK-deficient ($BK^{L1/L1}$; red) and wild-type ($BK^{+/+}$; blue) mice after 18 weeks of CD- (open bars) or HFD-feeding (filled bars). **(C)** CD and HFD food intake and **(D)** body core temperature, **(E)** activity and **(E)** tibia length of HFD-fed $BK^{+/+}$ and $BK^{L1/L1}$ at an age of 30 weeks. All data were evaluated using the Student's *t*-test and are presented as means ± SEM. Statistical difference between the two genotypes is indicated by ** P<0.01 or *** P<0.001.

***Suppl. Fig. 2:*** **(A)** BW gain of $BK^{+/+}$*; ob/ob* (n=19-22 mice per time-point, filled blue data points) and $BK^{L1/L1}$*; ob/ob* (n=11-18 mice per time-point, filled red data points) as well as the respective lean control littermates (*Lep +/+;* n=15-19 mice per time-point, open red or blue data points) fed a normal chow diet. **(B)** Body-composition of $BK^{+/+}$*; ob/ob* and $BK^{L1/L1}$*; ob/ob* mice at an age of 24 weeks was analyzed using the Soxhlet *extraction* method (n=4-5 mice per genotype). **(C)** Representative images of $BK^{+/+}$*; ob/ob* and $BK^{L1/L1}$*; ob/ob* mutants and their respective lean control littermates after a normal chow diet at an age of 24 weeks. **(D)** $BK^{+/+}$*; ob/ob* (n=17) and $BK^{L1/L1}$*; ob/ob* mice (n=13) and their lean control littermates (n= 9-12) fed a normal chow diet at an age of 24 weeks. Fat masses were normalized to tibia length (Suppl. Fig. 2E) to overcome the growth differences between the different *BK* genotypes that are not related to gain of body adiposity. Data were analyzed using the 2-way ANOVA test (C) or Student's t-test (B, D) and are presented as means ± SEM. Statistical difference between the two genotypes is indicated by * P<0.05, ** P<0.01, *** P<0.001. (**E**) Tibia length of male double-mutant $BK^{L1/L1}$*; ob/ob* (filled red bar; n=13) and $BK^{+/+}$*; ob/ob* control mice (filled blue bar; n=17) as well as lean $BK^{L1/L1}$*; Lep +/+* (open red bar; n=12) and $BK^{+/+}$*; Lep +/+* control mice (open blue bar; n= 9) at an age of 24 weeks. As expected, TL measurements confirm that the BK negative *ob/ob* and *Lep +/+* mice are smaller than their respective $BK^{+/+}$ controls. This difference, however, did not reach statistical significance for the lean groups. Number signs (#) indicate significant difference between $BK^{L1/L1}$; *ob/ob* and $BK^{L1/L1}$; *Lep +/+* mice suggesting that *BK/ob* influence each other in a complex manner. All data were evaluated using the Student's *t*-test and are presented as means ± SEM. Statistical difference is indicated by $***^{\#\#\#}$ P<0.001.

***Suppl. Fig. 3:*** **(A)** Epididymal white adipose tissue (eWAT) BK mRNA expression in BK wild-type ($BK^{+/+}$; n=6) and knock-out ($BK^{L1/L1}$; n=4) mice. Plus (+) reverse transcriptase (RT)

indicates samples for the quantification of BK mRNA levels. Minus (-) RT samples were analyzed in parallel in the absence of RT. **(B)** BK mRNA expression in inguinal WAT (iWAT) depot of $BK^{+/+}$ (n=5) and $BK^{L1/L1}$ (n=5) mice. **(C)** Immunohistochemical staining for BK (left panel) and hormone sensitive lipase (HSL; central panel) in cryosections of eWAT derived from $BK^{+/+}$ and $BK^{L1/L1}$ mice using 3,3'-Diaminobenzidine as a chromogen. Negative control staining without primary BK antibodies were processed in parallel and did not reveal a specific staining (right panel) in $BK^{+/+}$ or $BK^{L1/L1}$ eWAT. Scale bar = 200 µm. All data were evaluated using the Student's *t*-test and are presented as means ± SEM. Statistical difference between genotypes is indicated by * P<0.05, ** P<0.01, *** P<0.001.

***Suppl. Fig. 4:*** Upregulation of GLUT4 and BK channel (**A**) mRNA and (**B**) protein levels following differentiation of 3T3-L1 fibroblasts (pre-adipo) to adipocytes (adipo) (n =3/4 independent experiments per group). (**C**) Pre-adipo 3T3-L1 cells display no significant paxilline-sensitive (1µM) outward whole-cell BK potassium current determined under physiological potassium gradients (white; n = 8 cells). In contrast, paxilline-sensitive outward current was significantly increased in differentiated 3T3-L1 cells (black; n = 12 cells). (**D**) Inhibition of BK channels with paxilline (Pax) increased growth of differentiating 3T3-L1 cells (n = 4/group) compared to vehicle control (Ctr) and (**E**) increased adipogenic potential following 14 days of differentiation as determined by Oil-red-O (ORO) incorporation (n = 4/group). Data are Means ± SEM. * p<0.05 ANOVA with post-hoc Dunnett's test.

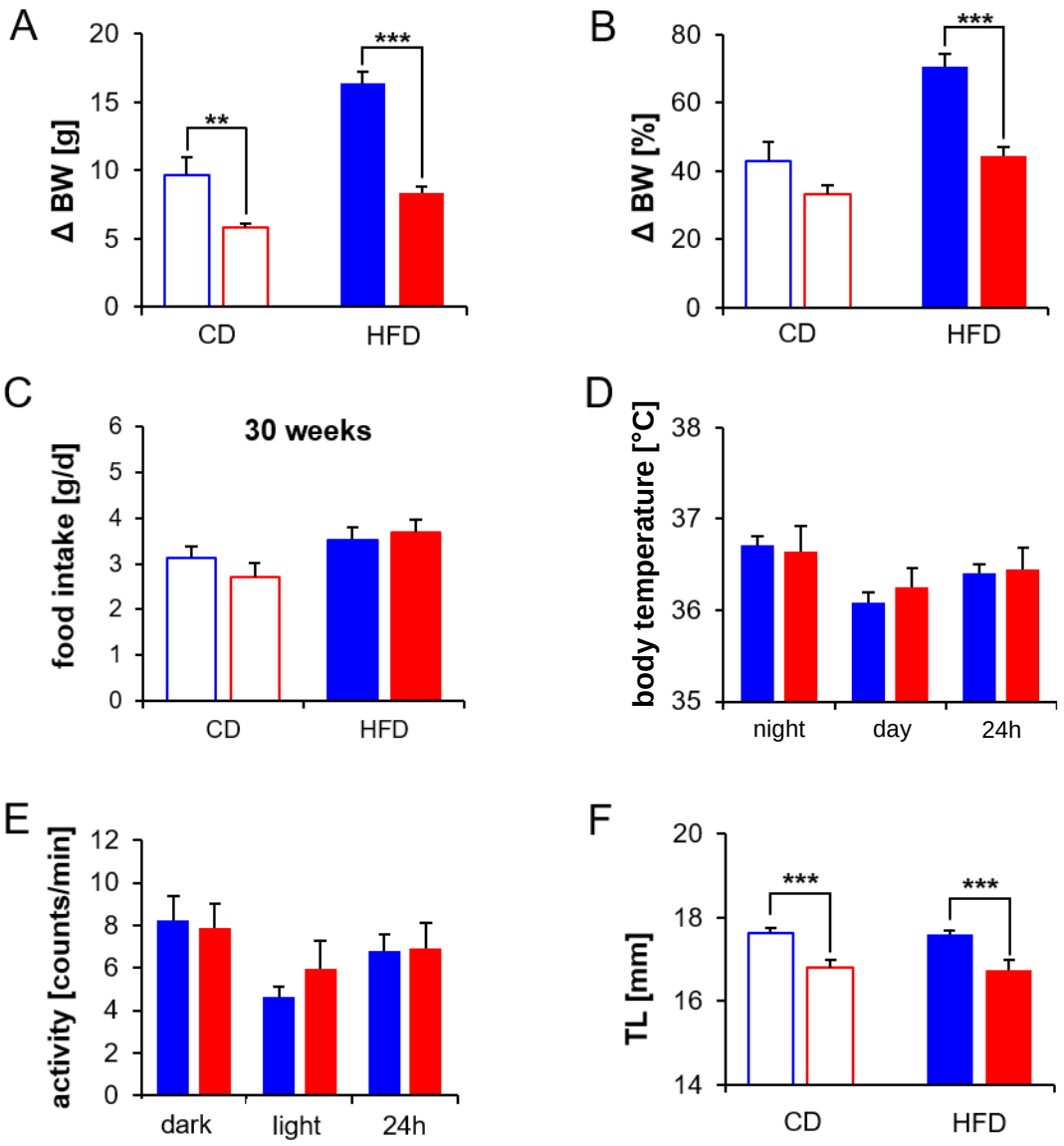
A
Δ BW [g]
20
15
10
5
0
**
***
CD
HFD
B
Δ BW [%]
80
60
40
20
0
***
CD
HFD
C
food intake [g/d]
30 weeks
6
5
4
3
2
1
0
CD
HFD
D
body temperature [°C]
38
37
36
35
night
day
24h
E
activity [counts/min]
12
10
8
6
4
2
0
dark
light
24h
F
TL [mm]
20
18
16
14
***
***
CD
HFD

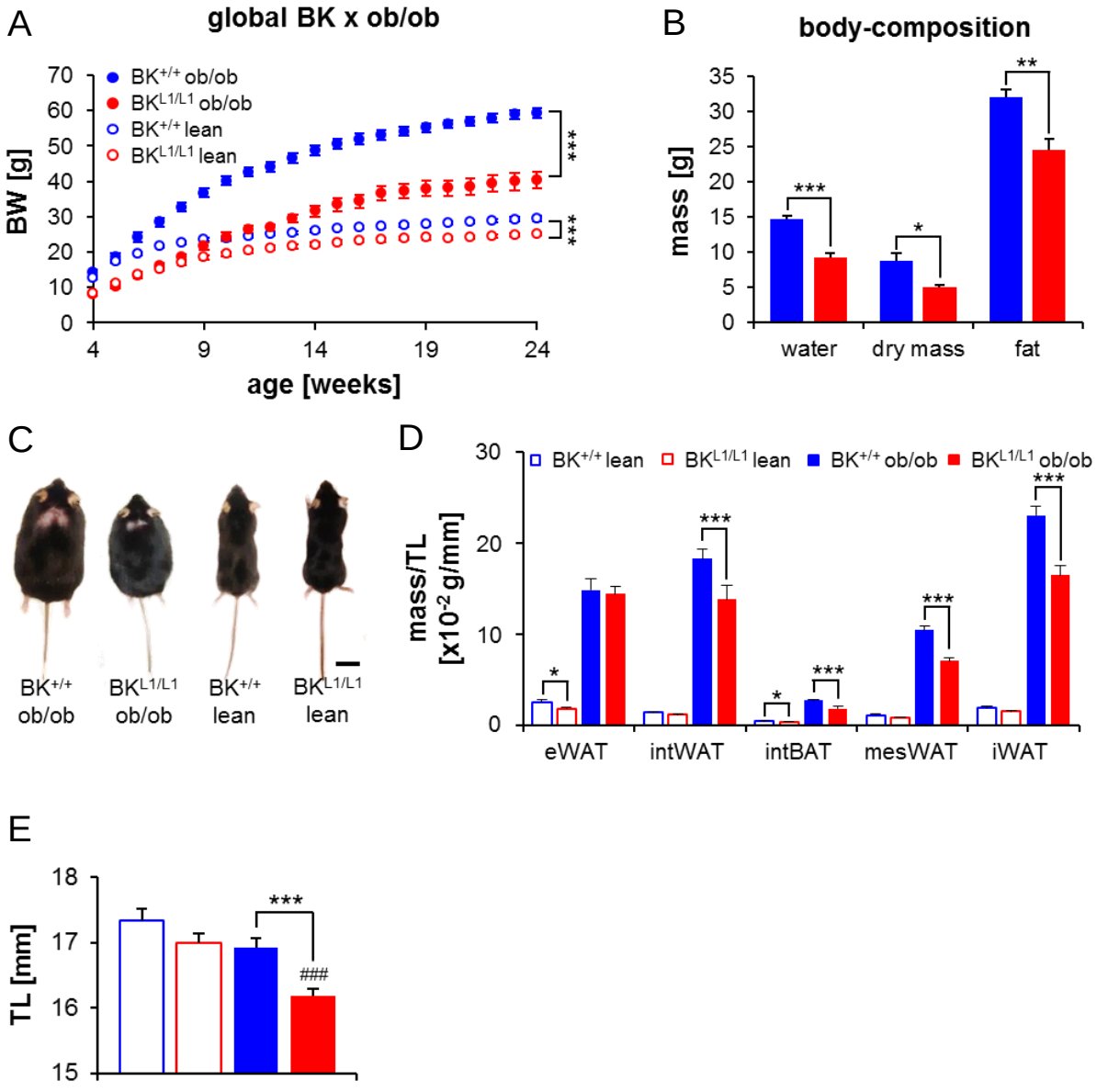
A
global BK x ob/ob
BW [g]
age [weeks]
BK+/+ ob/ob
BKL1/L1 ob/ob
BK+/+ lean
BKL1/L1 lean
***
***
B
body-composition
mass [g]
water
dry mass
fat
***
*
**
C
BK+/+ ob/ob
BKL1/L1 ob/ob
BK+/+ lean
BKL1/L1 lean
D
mass/TL [x10-2 g/mm]
BK+/+ lean
BKL1/L1 lean
BK+/+ ob/ob
BKL1/L1 ob/ob
eWAT
intWAT
intBAT
mesWAT
iWAT
E
TL [mm]
***
###

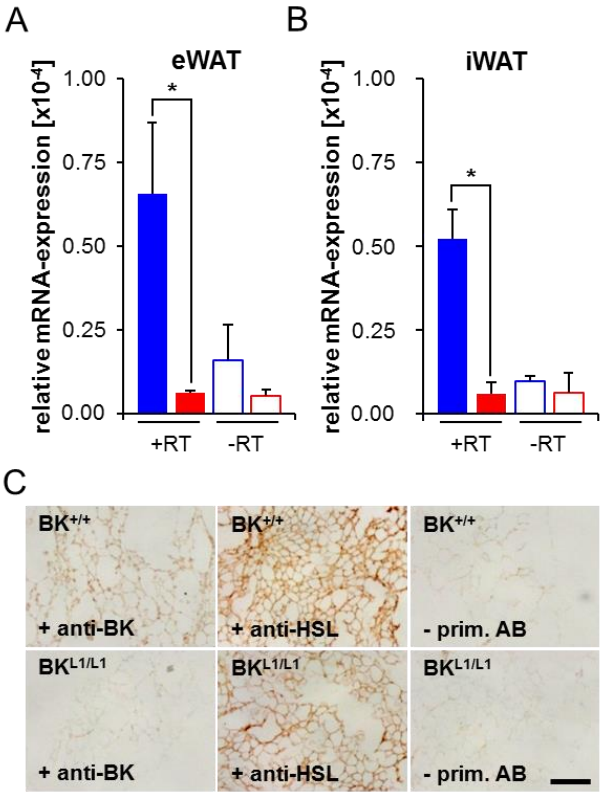
A
eWAT
relative mRNA-expression [x10⁻⁴]
1.00
0.75
0.50
0.25
0.00
*
+RT
-RT
B
iWAT
relative mRNA-expression [x10⁻⁴]
1.00
0.75
0.50
0.25
0.00
*
+RT
-RT
C
BK+/+
+ anti-BK
BK+/+
+ anti-HSL
BK+/+
- prim. AB
BKL1/L1
+ anti-BK
BKL1/L1
+ anti-HSL
BKL1/L1
- prim. AB

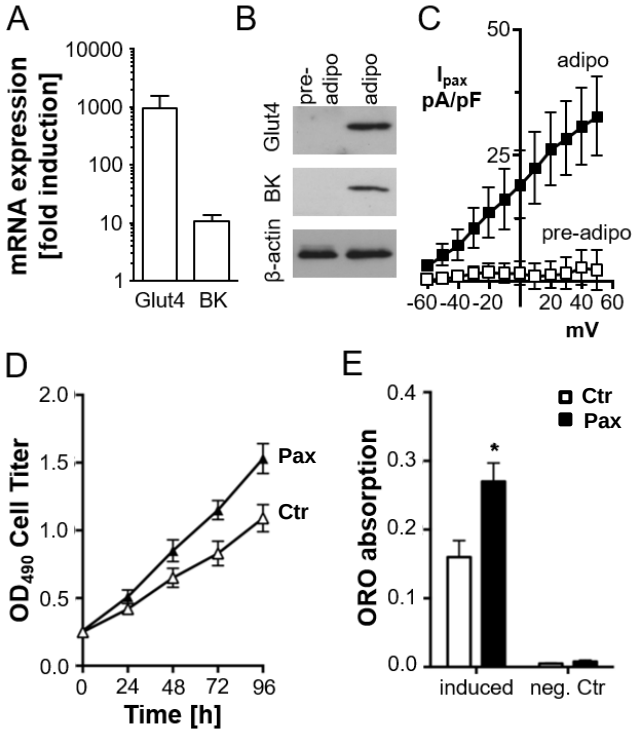
A
mRNA expression [fold induction]
10000
1000
100
10
1
Glut4
BK
B
pre-adipo
adipo
Glut4
BK
β-actin
C
$I_{pax}$ pA/pF
50
25
adipo
pre-adipo
-60 -40 -20
20 40 60
mV
D
$OD_{490}$ Cell Titer
2.0
1.5
1.0
0.5
0.0
Pax
Ctr
0
24
48
72
96
Time [h]
E
ORO absorption
0.4
0.3
0.2
0.1
0.0
Ctr
Pax
*
induced
neg. Ctr